Clays and Clay Minerals, Vol. 41, No. 2, 219–239, 1993.

CHLORITE GEOTHERMOMETRY: A REVIEW

PATRICE DE CARITAT,[1] IAN HUTCHEON,[1] AND JOHN L. WALSHE[2]

[1] Department of Geology and Geophysics, University of Calgary, Alberta, Canada T2N 1N4

[2] Department of Geology, Australian National University, Canberra, A.C.T. 2601, Australia

Abstract—Chlorite minerals, found in a great variety of rocks and geological environments, display a wide range of chemical compositions and a variety of polytypes, which reflect the physicochemical conditions under which they formed. Of particular importance for studies dealing with ore deposit genesis, metamorphism, hydrothermal alteration or diagenesis is the paleotemperature of chlorite crystallization. However, in order to understand the relationship between chlorite composition and formation temperature and hence use chlorite as a geothermometer, one must determine how other parameters influence chlorite composition. These parameters may include fO_2 and pH of the solution and Fe/(Fe + Mg) and bulk mineral composition of the host rock.

Four approaches to chlorite geothermometry, one structural and three compositional, have been proposed in the past: 1) a polytype method based on the (largely qualitative) observation that structural changes in chlorite may be partly temperature-dependent (Hayes, 1970); 2) an empirical calibration between the tetrahedral aluminum occupancy in chlorites and measured temperature in geothermal systems (Cathelineau, 1988), which has subsequently been modified by several workers; 3) a six-component chlorite solid solution model based upon equilibrium between chlorite and an aqueous solution, which uses thermodynamic properties calibrated with data from geothermal and hydrothermal systems (Walshe, 1986); and 4) a theoretical method based on the intersection of chlorite-carbonate reactions and the CO_2-H_2O miscibility surface in temperature-XCO_2 space, which requires that the composition of a coexisting carbonate phase (dolomite, ankerite, Fe-calcite or siderite) be known or estimated (Hutcheon, 1990). These four approaches are reviewed and the different calculation methods for the compositional geothermometers are applied to a selection of chlorite analyses from the literature. Results of this comparative exercise indicate that no single chlorite geothermometer performs satisfactorily over the whole range of natural conditions (different temperatures, coexisting assemblages, Fe/(Fe + Mg), fO_2, etc.). Therefore, chlorite geothermometry should be used with caution and only in combination with alternative methods of estimating paleotemperatures.

Key Words—Chlorite, Composition, Geothermometry, Polytype, Review.

INTRODUCTION

Chlorite, a mica-like clay mineral found in a variety of geological environments including sedimentary, low-grade metamorphic and hydrothermally altered rocks (Deer *et al.*, 1966), can either replace pre-existing (generally, ferro-magnesian) minerals or precipitate directly from solution. The ideal structure of this hydrous aluminosilicate is characterized by regularly alternating octahedral, "brucite-like" sheets (also known as the hydroxide sheets) and tetrahedral-octahedral-tetrahedral, "talc-like" sheets (also known as the 2:1 sheets) (e.g., see Bailey, 1988a). The mineral displays a wide range of composition and a general crystallochemical formulation for chlorite has been suggested to be:

$$(R^{2+}_u R^{3+}_y \square_z)^{VI}(Si_{4-x}Al_x)^{IV}O_{10+w}(OH)_{8-w} \qquad (1)$$

(modified from Wiewióra and Weiss, 1990), where $u + y + z = 6$, $z = (y - w - x)/2$, w generally is zero or a small number, R^{2+} generally represents Mg^{2+} or Fe^{2+}, R^{3+} generally represents Al^{3+} or Fe^{3+}, and $\square$ represents structural vacancies. Octahedral sites (superscript VI) are differentiated from tetrahedral sites (superscript IV) in this general formula. Octahedral occupancy represents the sum of all cations in the octahedral site, and is given by $\Sigma^{VI} = u + y$. Figure 1 illustrates how chlorite compositions can be plotted in terms of the major cations, Si, Al, Fe, and Mg.

Not represented in Eq. 1 are components that commonly occur in minor amounts in the octahedral site of chlorite, such as Cr, Ti, Ni, Mn, V, Cu, and Li. These, together with the major chlorite constituents Mg, Fe^{2+}, Fe^{3+}, Al, and Si, contribute to the wide-ranging compositional variability, or non-stoichiometry, that makes chlorite a potentially attractive geothermometer. By virtue of this non-stoichiometric behavior, chlorite has the potential to record invaluable information about the physicochemical conditions under which it formed. It has been observed, for instance, that the effects of increasing burial depth, metamorphic grade, or hydrothermal alteration upon chlorite composition include a decrease in Si^{IV}, Al^{VI}, and $\square^{VI}$ and an increase in Al^{IV}, (Fe + Mg), and Σ^{VI}.

In addition to compositional changes, structural changes have been noted to occur in natural chlorites, and these polytype transitions have been suggested to depend on ambient temperature as well. Chlorite polytypism is, therefore, included in the present general review of chlorite geothermometry, and this subject is also covered by Walker (this issue).

Several workers have attempted to design more or less sophisticated tools to translate chlorite compositions (and polytype occurrences) into paleotemperature readings, a most legitimate and commendable, if intricate, exercise. These efforts have yielded acceptable results in limited cases, but there still exists a justified lack of confidence in applying these geothermometers to widely different data sets. The present paper briefly summarizes and compares results of these methods. Before discussing further the issue of chlorite geothermometry, however, it is useful to review polytypism and compositional range of natural chlorites.

CHLORITE POLYTYPISM

The manner in which hydroxide and 2:1 sheets are stacked in the z-direction defines the polytype of chlorite. There are numerous possible ways in which to conceive such stacking sequences, and these are derived by varying the position and orientation of the hydroxide interlayers about fixed 2:1 layers. Bailey and Brown (1962) showed six theoretically possible layer-interlayer assemblages, or 14 Å structural units, in either semi-random or in regular "one-layer" polytypes. Of these six polytypes, four have been observed in nature: II*b*, I*b* (β = 90°), I*b* (β = 97°), and I*a* (in decreasing order of known abundance; see Walker, 1989). In practice, semi-random chlorite polytypes (comprising most chlorites) are identified on the basis of the position of (*h0l*) reflections in random X-ray powder photographs obtained with a Debye-Scherrer camera (see Bailey, 1984). Hayes (1970) proposed an additional stacking arrangement for a highly disordered chlorite, Ib_d, exhibiting strong (00*l*) reflections and lacking (*h0l*) reflections. For a more complete discussion of chlorite polytypism, the reader is referred to Bailey and Brown (1962), Brown and Bailey (1963), Shirozu and Bailey (1965), Lister and Bailey (1967), Hayes (1970), and Bailey (1984, 1988a, 1988b).

COMPOSITIONAL VARIABILITY OF CHLORITES

Much of the classic literature dealing with chlorite composition and classification schemes is based on chlorites from metamorphic or hydrothermal environments (Hey, 1954; Foster, 1962).

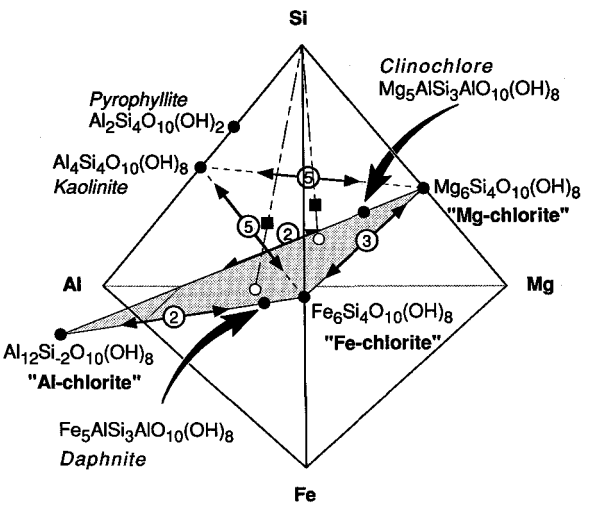

Figure 1. Si-Al-Fe-Mg tetrahedron for representation of chlorite analyses (solid squares). Plane (stippled) intersecting the tetrahedron is used for ternary "Al-chlorite," "Fe-chlorite," "Mg-chlorite" diagrams. Positions of chlorite analyses in this plane (open circles) are obtained by projection through the Si apex (dashed lines). Circled numbers with arrows refer to exchange reactions and vectors of Table 1.

One of the most common substitutions in chlorites is that of the type $Mg^{VI}Si^{IV} \leftrightarrow Al^{VI}Al^{IV}$ (hereafter referred to as the "Tschermak exchange"; see exchange 2 in Figure 1 and Table 1), which leads to a redistribution of charges between the tetrahedral and octahedral layers but maintains overall charge balance. Theoretically, tetrahedral substitution of Si^{4+} by Al^{3+} via a Tschermak exchange should be accompanied by an equivalent amount of octahedral substitution of R^{2+} by Al^{3+} in order to conserve charge balance, and, therefore, the values of Al^{IV} and Al^{VI} should be equivalent. Although these appear to be positively correlated overall, the value of Al^{VI} in naturally occurring chlorites is commonly either somewhat greater or smaller than the value of Al^{IV} (Foster, 1962), indicating that other substitutions take place. If $Al^{VI} > Al^{IV}$, then the octahedral R^{3+} in excess of Al^{IV} may be interpreted as having replaced R^{2+} in a 2:3 ratio. Conversely, if $Al^{VI} < Al^{IV}$, then additional octahedral R^{3+}, in the form of Fe^{3+} for instance, may be interpreted as having replaced Al^{VI} in a 1:1 ratio.

Table 1. Chlorite components and exchange reactions (from Walshe, 1986).

	Oxide component	Molecular component	Exchange reaction	Exchange vectors
1	SiO_2	$Mg_6Si_4O_{10}(OH)_8$	—	—
2	MgO	$Mg_5AlSi_3AlO_{10}(OH)_8$	$(Si^{4+})^{IV}(Mg^{2+})^{VI} \leftrightarrow (Al^{3+})^{IV}(Al^{3+})^{VI}$	$Al_2Si_{-1}Mg_{-1}$
3	FeO	$Fe_5^{2+}AlSi_3AlO_{10}(OH)_8$	$(Mg^{2+})^{VI} \leftrightarrow (Fe^{2+})^{VI}$	$FeMg_{-1}$
4	Fe_2O_3	$Fe_5^{2+}Fe^{3+}Si_3Fe^{3+}O_{10}(OH)_8$	$(Al^{3+})^{VI} \leftrightarrow (Fe^{3+})^{VI}$	$Fe^{3+}Al_{-1}$
5	Al_2O_3	$Al_4\square_2Si_4O_{10}(OH)_8$	$3(Mg,Fe^{2+})^{VI} \leftrightarrow 2(Al^{3+})^{VI}\,\square^{VI}$	$Al_2(Mg,Fe^{2+})_{-3}$
6	H_2O	$Fe_4^{2+}Fe^{3+}AlSi_3AlO_{11}(OH)_7$	$(Fe^{2+})^{VI}2(OH)^- \leftrightarrow (Fe^{3+})^{VI}O^{2-}(OH)^-$	$Fe^{3+}O^{2-}Fe^{2+}_{-1}OH_{-1}$

https://doi.org/10.1346/CCMN.1993.0410210 Published online by Cambridge University Press

An indication of the extent of tetrahedral substitution of Si by Al in natural chlorites is given by the observed range of tetrahedral compositions. Foster (1962) found that Si^{IV} values from a compilation of about 150 chlorite analyses fell between 2.34 and 3.45, with 99% of these values falling within the 2.40–3.40 range. Thus, the value of x in Eq. 1 varies mostly between 0.6 and 1.6 in metamorphic/hydrothermal chlorites.

An additional complexity in the crystallochemical definition of chlorites is the distribution of the cations and their substitutions between the two octahedral layers, the "brucite-like" octahedral interlayer, and the octahedral layer within the "talc-like" sheet. Foster (1962) speculated that cations are most likely to be equally distributed between the two octahedral layers. At odds with this, Wiewióra and Weiss (1990), reviewing the literature on single crystal studies of trioctahedral chlorites (the most abundant type of naturally occurring chlorites), concluded that Al is concentrated primarily in the interlayer hydroxide ("brucite-like") sheet.

Foster (1962) found that octahedral vacancies commonly account for between 0.0 and 0.3 positions but may range from −0.05 to 0.55 positions per $O_{10}(OH)_8$ (half-cell structure). As stated in Eq. 1, the number of octahedral vacancies, z, varies proportionally to $(y - w - x)$, the difference between $(R^{3+})^{VI}$, O in excess of 10.00, and Al^{IV}.

Hey (1954) suggested that chlorites be subdivided into "oxidized chlorites" and "unoxidized chlorites," depending on whether they contain more or less than 4 wt. % Fe_2O_3, respectively. Chlorite analyses compiled by Foster (1962) indicate an extent of Fe_2O_3 content up to 20.18 wt. %, which usually increases as the Fe^{2+}: R^{2+} atomic ratio increases. Foster (1962) found no correlation between Fe_2O_3 and O content in excess of 10.00 ions per half-cell (w in Eq. 1), as would be expected if Fe^{2+} in chlorites was oxidized. Furthermore, she argued that some or all of the Fe^{3+} present is necessary for structural balance in many chlorites and pointed out that many chlorites are formed by alteration of other minerals which may contain Fe^{3+}. This led her to conclude that Fe_2O_3 is a normal constituent of many chlorites, particularly ferroan chlorites, and that its presence should not be interpreted as evidence for secondary oxidation. Particularly, octahedral cation totals in excess of 6.00 per half-cell when all Fe is taken to be ferrous is strong evidence that part of the iron is ferric (Foster, 1962). Most chlorites in which the Fe^{2+}:R^{2+} ratio is less than 0.45 contain less than 4 wt. % Fe_2O_3, whereas chlorites in which this ratio is greater than 0.45 generally contain more than 4 wt. % Fe_2O_3, although some may contain less (Foster, 1962).

In terms of charge balance of the chlorite structure (charge balance = $2u + 3y - x - w - 12$; see Eq. 1), all of Foster's data fall within the range −0.05 to +0.05, with 94% of those data falling within the smaller range −0.03 to +0.03 per half-cell structure.

Inasmuch as the non-stoichiometric behavior of chlorite must be somewhat idealized for the purpose of its analysis, it will be assumed that the relationships between u, w, x, y and z given in Eq. 1 must be obeyed for any particular chlorite formula, and so must the charge balance equation.

DIAGENETIC CHLORITES

Chlorites from low-temperature environments, such as those found in sedimentary rocks from the diagenetic to low-grade metamorphic realms, exhibit some compositional differences compared to higher-grade metamorphic or hydrothermal chlorites (Curtis *et al.*, 1985). For instance, diagenetic (or sedimentary) chlorites tend to have higher Si contents and lower (Fe + Mg) contents and octahedral totals than metamorphic chlorites of similar alumina content (Curtis *et al.*, 1985; Hillier and Velde, 1991). During the passage from diagenesis to metamorphism thus, chlorites apparently become less siliceous, richer in (Fe + Mg), and octahedral occupancy increases; and this transition must be accompanied by an increase in Al^{IV} and a decrease in Al^{VI} if aluminum is to be conserved at the chlorite structure scale (Hillier and Velde, 1991). Using transmission electron microscope (TEM) results, Jahren (1991) documented increasing Al/Si ratios from core to rim in diagenetic chlorites having grown during progressive burial and heating, and he suggested that growth of these chlorites was controlled by a grain coarsening process related to Ostwald ripening. In parallel with these chemical changes, sedimentary chlorites undergo polytype evolution with increasing diagenetic grade (see below).

In analyzing chlorites from the diagenetic realm, one often is confronted with the problems of chlorite interlayering and compositional purity. In a review of the literature, de Caritat and Walshe (1990) indicated that many reported chlorites from low-temperature settings are indeed commonly interstratified with smectite, vermiculite, saponite, and/or illite. The resolution of the electron microprobe, the most commonly used analytical instrument for acquiring mineral compositional data on chlorites, does not allow the user to ascertain directly the purity of the "chlorite" analyzed. In an attempt to reject results presenting obvious flaws, many authors have discarded analyses in which the total Ca, Na, and K oxides exceeds 0.5 wt. % (Foster, 1962; Velde and Medhioub, 1988) based on the argument that there is no room for these elements in the chlorite structure. Ultimately, one would like to verify the purity of chlorite at the scale of the structure itself, and pioneering analytical TEM work on North Sea chlorites by Jahren and Aagaard (1989) presents invaluable advantages in this regard.

DESCRIPTION OF CHLORITE NON-STOICHIOMETRY AND CALCULATION OF COMPONENT MOLE FRACTIONS

The wide compositional variability of chlorite can be represented graphically by a tetrahedron volume with Si, Al, Fe, and Mg as apices (Figure 1). Projections in hyperspace would allow representation of more components of chlorite but are not amenable to three-dimensional visualization. For the purpose of comparing chlorite compositions in an even more practical fashion, one can project the composition of any chlorite in the tetrahedron of Figure 1 through one apex—for instance, Si—and thus represent the point where that projection goes through a selected plane. In Figure 1, we chose a plane for projection (stippled) that has "Mg-chlorite" ($Mg_6Si_4O_{10}(OH)_8$) and "Fe-chlorite" ($Fe_6Si_4O_{10}(OH)_8$) as two of the three corners, since these are the most Mg-rich and Fe-rich "chlorites," respectively, and are thus suitable as end-members. To select the third corner or end-member, we imposed that the plane pass through the compositional locus of two common chlorites, clinochlore ($Mg_5AlSi_3AlO_{10}(OH)_8$), and daphnite ($Fe_5AlSi_3AlO_{10}(OH)_8$). The calculated third apex thus found is $Al_{12}Si_{-2}O_{10}(OH)_8$, which represents a hypothetical "Al-chlorite" composition analogous to the aluminous biotite proposed by Rutherford (1973). Because neither of these three end-member chlorite compositions have actually been found in nature, their names are here given within quotation marks. Plotting chlorite compositions in the "Fe-chlorite," "Mg-chlorite," and "Al-chlorite" plane has significant practical advantages in terms of visualization over higher-dimension representations, but some information (e.g., proportions of Si, Fe^{3+}, minor components) is lost in the process.

Most published analyses of chlorite are obtained using the electron microprobe, a technique that yields information on the extent of the Tschermak exchange, the Mg-Fe exchange, and the "di-tri" exchange (exchange reactions 2, 3, and 5, respectively, see Figure 1 and Table 1), but does not yield information on the Fe^{2+}:Fe^{3+} ratio or on the water content (H_2O^+, H_2O^-) of the mineral. However, where the cation total (CAT $= u + y + 4$, see Eq. 1) exceeds the maximum permitted value (10.00, for a half-cell formula, Eq. 1), an indirect method for estimating the *minimum* amount of Fe^{3+} substitution for Al^{3+} in the octahedral site exists (Walshe, 1986). This method is based on the ratio 10/CAT, which is the factor required to reduce the cation total to the theoretical maximum. The minimum estimate of Fe^{3+} ions is given by the relation 28 (1 − 10/CAT), and the number of all other cations must be reduced by 10/CAT.

Walshe (1986) used a set of six molecular components, given in Table 1, to describe the composition of any chlorite within the six-component system SiO_2, Al_2O_3, FeO, Fe_2O_3, MgO and H_2O. As thermodynamic components, six molecular components would be equivalent to the six oxide components. There is an element of choice in selecting the actual composition of each component, but, importantly, the six are linearly independent, i.e., the composition of one of these components cannot be described in terms of the composition of any of the others. This point may be appreciated by comparing the list of molecular components given in Table 1 with the adjacent list of exchange reactions. The six components may be considered equivalent to one additive component and five exchange vectors, after Thompson (1982).

Walshe (1986) determined the mole fractions of the six molecular components (X1, X2, . . . , X6) of Table 1 from the cation concentrations in the half-cell formula (Eq. 1) by utilizing six mass conservation equations (see Walshe, 1986, Table 10B). However, assuming no ferric iron (X4 = 0) and normal water content (X6 = 0) in the chlorite structure, a common starting point, these six equations reduce to the following five equations:

$$Mg = 6X1 + 5X2, \quad (2)$$

$$Si = 4(X1 + X5) + 3(X2 + X3), \quad (3)$$

$$Al = 2(X2 + X3) + 4X5, \quad (4)$$

$$Fe = 5X3, \quad \text{and} \quad (5)$$

$$\square = 2X5 = 10 - CAT, \quad (6)$$

where Al represents the total aluminum (octahedral plus tetrahedral). From this set of equations, the mole fraction of the molecular components can be derived:

$$X1 = Mg/6 - 5X2/6 \quad (7)$$

$$X2 = Al/2 - X3 - 10 + CAT \quad (8)$$

$$X3 = Fe/5 \quad (9)$$

$$X5 = (10 - CAT)/2. \quad (10)$$

There are five constraints (Eqs. 2–6) and only four unknowns (Eqs. 7–10), reflecting a dependency in the equation set generated by the fact that the total cation charge is fixed at 28 for the half-cell formula if X6 is zero. Thus, the cation abundances are related by:

$$2(Mg + Fe) + 4\,Si + 3\,Al = 28. \quad (11)$$

RELATIONSHIPS BETWEEN CHLORITE, FLUID, AND BULK ROCK COMPOSITIONS

The composition of a grain of chlorite that grows as a fluid interacts with a rock will be determined by a number of factors, including temperature, pressure, bulk rock composition, fluid composition, and rate of mineral growth. Assuming that fluid-mineral equilibrium is maintained during the growth of chlorite, classical thermodynamics allows us to describe the composition

of the growing grain in terms of the composition of the aqueous fluid, temperature and pressure. The aqueous solution variables are equivalent in number to the oxide components or the molecular components (Table 1) used to describe chlorite compositions. Again, there is an element of choice regarding these variables; the set selected by Walshe (1986) is T, P, aH_2O, aH_4SiO_4, $aAl^{3+}/(aH^+)^3$, $aMg^{2+}/(aH^+)^2$, $aFe^{2+}/(aH^+)^2$ and fO_2, where a is activity and f is fugacity. Classical thermodynamics does not necessarily give us an insight into what controls the values of these variables. If water : rock ratios are high, it may be the fluid composition; if water : rock ratios are low, it may be the bulk composition of the rock. In situations where there is some net transport of matter, it is likely that the fluid controls at least some of these variables.

The importance of bulk rock composition/mineralogy upon chlorite composition (Albee, 1962) often has been neglected in previous studies of chlorite geothermometry and perhaps requires some further discussion and research. An analogy between chlorite and biotite illustrates this point.

Past work shows that the composition of biotite in metamorphic or igneous rocks is influenced by the bulk rock mineralogy of the hosting medium (Nockolds, 1947). Engel and Engel (1960) have shown that biotites become increasingly MgO-rich (more phlogopite-like) and (FeO,MnO)-poor (less annite-like) in rock types evolving from pegmatites to granites, gneisses and schists, diorites, gabbros and basalts, ultramafics, and marbles. Temperature (metamorphic grade) *and* bulk rock composition/mineralogy thus both affect biotite composition.

In chlorites, it has been shown that the Fe/(Fe + Mg) ratios of chlorite and bulk host rock are directly proportional to each other (Cathelineau and Nieva, 1985, Figure 6; Bevins *et al.*, 1991, Figure 2), indicating at least some bulk rock compositional control. As is the case for biotite, it is likely that bulk rock mineralogy or composition will exercise some control over the composition of chlorite.

The relationship between fO_2, host rock mineral assemblage, and Fe:Al:Mg ratio of chlorite is illustrated in Figure 2, which is analogous to a similar ternary diagram for biotites (Hutcheon, 1977). Accepting the premise of crystal growth under fluid-mineral equilibrium conditions, the composition of chlorites precipitating at some constant temperature and pressure in rocks of increasing aluminum content will, by definition, be in equilibrium with more and more aluminous mineral assemblages. For instance, mineral assemblages may evolve from K-feldspar alone to K-feldspar + smectite, to smectite, to smectite + illite, to illite, to illite + kaolinite, to kaolinite, to kaolinite + gibbsite, to gibbsite (Figure 2). The Fe:Mg ratio of chlorite coexisting with any of these silicate assemblages at any fixed temperature and pressure is directly related to fO_2. This anticipated relationship between bulk rock composition/mineralogy and chlorite composition is particularly important when one considers that some geothermometers directly relate Al^{IV} in chlorite to precipitation temperature (e.g., Cathelineau and Nieva, 1985; Cathelineau, 1988). This is not to say that Al^{IV} will not vary with precipitation temperature. Rather, the above discussion stresses the fact that aluminum content variations are likely to be singularly related to temperature effects *only within one particular type of bulk rock mineralogical assemblage* and that *different Al^{IV}-temperature relationships are likely to be found in different rock types.* Thus, the question that one must ask is: How important is the bulk rock composition/mineralogy control upon chlorite composition compared to the temperature control? If the former is found to have a significantly subordinate role compared to the temperature control, then a unique chlorite composition-temperature relationship based on aluminum content can be applied to a variety of rock types. Otherwise, this relationship will have to be lithology-dependent. More work on this aspect of chlorite geothermometry—and indeed any other type of mineral geothermometry—will shed some light on this important question.

CHLORITE GEOTHERMOMETRY

The non-stoichiometric behavior of chlorite makes it a potentially attractive geothermometer, as chlorite composition records invaluable information about the physicochemical conditions prevailing during its formation. The condition for this compositional geothermometer to perform satisfactorily is that it should be possible to unequivocally relate chlorite composition to temperature of formation. Three main approaches to this problem have been presented, and these will be briefly reviewed hereafter. First, however, we will explore how the chlorite structure varies with temperature, and, thus, how chlorite polytypism may be used as a geothermometer (see also Walker, this issue).

POLYTYPE GEOTHERMOMETRY

Bailey and Brown (1962) determined the polytype of more than 300 natural chlorites, 80% of which were II*b* and occurred in metamorphic and igneous rocks and higher temperature ore deposits, while the remaining 20% were of the three type-I polytypes and were reported (p. 845) to ". . . occur in geologic environments or in mineral associations that suggest a lower temperature-pressure energy level than that for II*b* chlorite." Hayes (1970) analyzed chlorites from sedimentary rocks and concluded that there is a natural polytype progression with temperature from Ib_d to I*b* ($\beta = 97°$), to I*b* ($\beta = 90°$), to II*b*, which reflects increasing polytype stability. Most type-I chlorites, Hayes suggested, are of authigenic origin and form under temperature and pressure conditions less than those of

low-grade metamorphism. Therefore, Hayes (1970) concluded that clay-size II*b* chlorite in unmetamorphosed sedimentary rocks can be interpreted as detrital, although he warned that this polytype may form during diagenesis at "submetamorphic" temperatures because it is the most stable arrangement. The transition from I*b* (β = 90°) to II*b*, which requires the rotation of the interlayer hydroxide sheet, however, was inferred to generally require temperatures of about 150°–200°C (Hayes, 1970). Chlorite composition was found to be of subordinate importance to temperature in polytype evolution.

Karpova (1969) documented the transition from Fe 7Å I*b* (β = 90°) chlorite to Fe 14 Å I*b* (β = 90°) chlorite, to Mg-Fe 14 Å II*b* chlorite within terrigenous Carboniferous rocks from Bolshoy Donbas as a function of increasing burial. This study, therefore, documents the relationship between transition from type-I to type-II chlorites and increasing diagenetic grade and qualitatively reports a parallel compositional change (loss of Fe and enrichment in Mg). Although no temperature values were given, Karpova (1969, Figure 10) indicated that the maximum burial depth experienced by the I*b* chlorite zone was 3–4 km.

Weaver *et al.* (1984) reported the persistence of polytype I*a* at speculated temperatures as high as 250°–300°C from the study of a suite of diagenetic/metamorphic rocks (shale-to-slate transition) in the southern Appalachians. Polytype II*b* was found in a sample subjected to metamorphic temperatures of the order of 330°C, and it could not be shown that this chlorite had formed directly from the I*a* polytype. On the basis that chlorite polytype I*a* may be stable at intermediate temperatures (150°–300°C), the authors suggested that it may be more common in sedimentary rocks at these temperatures than previously recognized.

Curtis *et al.* (1985) analyzed a series of authigenic chlorites in sandstones from several sedimentary basins (North Sea, Western Canada Sedimentary Basin, Gulf Coast), both in terms of polytypes and in terms of chemical composition. In agreement with Hayes (1970), they concluded that grain-coating chlorites in sandstones are mostly polytype I*b* (β = 90°), and that they are more siliceous and Fe-rich than metamorphic chlorites (polytype II*b*), a conclusion not reached by Hayes on the basis of X-ray diffraction data. They proposed a possible evolutionary pathway (Curtis *et al.*, 1985, Figure 8) for chlorite in sedimentary basins: swelling chlorite [$Si^{IV} > \sim 3.25$; $0.4 < Fe/(Fe + Mg) < 0.7$] develops from smectite and, with progressive burial, is converted first to polytype I*b* (β = 90°) [$Si^{IV} \approx 3$; $0.4 < Fe/(Fe + Mg) < 0.85$] then to polytype II*b* [$Si^{IV} < \sim 3$; $0 < Fe/(Fe + Mg) < 1$]. Alternatively, sedimentary chlorite may start as a berthierine [$Fe/(Fe + Mg) > 0.8$] and evolve directly into chlorite polytype II*b*. Curtis *et al.* (1985) noted, however, that the best-described chlorites do not seem to have developed by either of these mechanisms, but rather appear to have grown directly from precipitation out of the pore fluid (neoformation) to form grain coatings in sandstones. No temperature information is given, but the deepest [presumably I*b* (β = 90°) polytype] chlorites reported in Curtis *et al.* (1985) are from depths of about 5600 m (Tuscaloosa Sandstone).

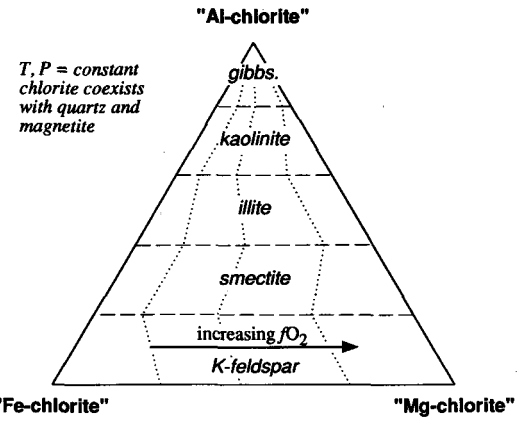

Figure 2. Schematic diagram illustrating how coexisting mineral assemblage and fO_2 will, in theory, influence the composition of a growing chlorite, in terms of the three main chlorite end-members, "Al-chlorite," "Fe-chlorite" and "Mg-chlorite" (see Figure 1). At any given *T*, *P* and fO_2, chlorite growing in coexistence with quartz, magnetite, and with one or two minerals from the series K-feldspar, smectite, illite, kaolinite or gibbsite, will have an increasing "Al-chlorite" content depending on how aluminous the bulk mineral assemblage is (increasingly aluminous from K-feldspar to gibbsite). The Fe:Mg ratio of chlorite is dictated by fO_2. This figure illustrates the dependency of chlorite composition on bulk rock composition/mineralogy and fO_2 upon which the effects of temperature and pressure are superimposed in natural settings. Positions of the various mineral field boundaries are schematic.

Whittle (1986) determined polytypes of pore lining chlorites in sandstones, using XRD and TEM, on a dataset apparently partly overlapping with the one used by Curtis *et al.* (1985). In all cases where polytype determination was possible, polytype I*b* (β = 90°) was identified. No indication of temperature, however, is given.

In an investigation of chlorite polytypism in very-low-grade metamorphic rocks from Maine, Walker (1989) exclusively found II*b* chlorites. Because II*b* chlorite was present in both the fine-grained metasedimentary and the metavolcanic rocks studied, a detrital source as sole origin for the chlorite was ruled out. Walker (1989) concluded that chlorite II*b* must have largely formed and/or recrystallized *in situ* and that the minimum temperature at which this polytype is stable is therefore equivalent to the minimum temperature of metamorphism of the host rock. This minimum metamorphic temperature was estimated to have been between 50°C (based on conodont colors) and 150°C (based on mineral assemblages). Walker (1989) spec-

ulated that the reasons for the discrepancy between his observations and Hayes' (1970) statement may be that, in fine-grained rock, polytype transformations depend not only on temperature, but also on pore pressure and time.

Similarly, chlorite in the <0.5-μm fraction separated from a fine-grained sequence undergoing diagenesis in the Imperial Valley was found to be exclusively of type II*b* (Walker and Thompson, 1990). Minimum temperature of the sampled interval was 135°C, leading Walker and Thompson (1990) to argue that transition from polytype-I to stable polytype-II in fine-grained rocks may occur at temperatures lower than first suggested by Hayes (1970).

Hillier (this issue) shows that authigenic chlorite II*b* formed during the diagenetic alteration of a suite of lacustrine mudrocks from the Devonian Orcadian Basin of Scotland. Paleotemperatures of chlorite formation are inferred to have been as low as 120°C. Mechanism of chlorite formation in this case is suggested to have involved the reaction of dolomite with illite to produce chlorite and calcite, similar to that reported by Hutcheon (1990).

Chlorite polytype geothermometry appears thus to require more detailed studies on what controls the transition from type-I to type-II in nature (see Walker, this issue). In the above review of polytype geothermometry, only two studies (Karpova, 1969, and Weaver *et al.*, 1984) actually document this transition; all other reported studies have found only one polytype. The effect of grain size of the host rock appears to be a fundamental control, and this warrants further systematic investigation.

THE EMPIRICAL CALIBRATION

Numerous workers have noted a systematic decrease in Si^{IV} (or conversely an increase in Al^{IV}) and a decrease in $\square^{VI}$ (or conversely an increase in Σ^{VI}) in chlorites with increasing depth in diagenetic and geothermal systems or with increasing grade of metamorphism in metamorphic rocks (McDowell and Elders, 1980; Cathelineau and Nieva, 1985; Cathelineau, 1988; Jahren and Aagaard, 1989; Hillier and Velde, 1991). Some authors have reasoned that these mineralogical changes result from the progressive increase in the temperature of chlorite formation.

Cathelineau and Nieva (1985) studied the geothermal system of Los Azufres, Mexico, where chlorite constitutes a major hydrothermal alteration product of the andesitic host rock. Chlorite compositions were determined by electron microprobe analysis of samples from different depths within a series of wells. The temperature of chlorite crystallization was estimated either from downhole measurements and from aqueous geothermometers (assuming that present-day temperature closely approximates crystallization temperature) or from microthermometric data on fluid inclusions found in coexisting phases (e.g., quartz). It varies between 130° and 310°C over the sampled depth range (Cathelineau, 1988). Cathelineau and Nieva (1985) found a positive correlation between Al^{IV} and temperature and suggested that Al^{IV} could be used as a geothermometer in this system, since no other thermodynamic parameter (bulk rock composition, nature of geothermal fluids, pressure) appears to vary significantly there. [Note that, as full tetrahedral occupancy in chlorites is only an assumption, it may be more significant to utilize the quantity Si^{IV}, rather than Al^{IV}, which is calculated from the difference between tetrahedral occupancy (4, or less?) and Si^{IV}.]

Based on new chlorite analyses and fluid inclusion data from Los Azufres, and data from the Salton Sea (recalculated and averaged from McDowell and Elders, 1980), Cathelineau (1988) derived the following relationship between temperature, T (°C), and Al^{IV}:

$$T = -61.92 + 321.98\ Al^{IV}. \quad (12)$$

Cathelineau (1988) suggested that Eq. 12 has the potential to be used as a chlorite geothermometer of general applicability in diagenetic, hydrothermal, and metamorphic settings because the value of Al^{IV} appears to be independent of rock lithology [it fits both andesitic (Los Azufres) and feldspathic sandstone (Salton Sea) lithologies] and fluid composition. Bevins *et al.* (1991), for instance, have used the Cathelineau (1988) expression to derive calculated temperatures of chlorite formation in metabasites from Wales and Greenland. Velde *et al.* (1991) cautioned that the Los Azufres data presented in Cathelineau and Nieva (1985) shows notable quantities of Ca and K and exhibits a correlation between minor and major element abundances. This indicates, they argued, that the composition of the phases is due not to the physical conditions claimed by the authors, but to the phase association present (interstratified chlorite/smectite?). The revised chlorite data from Los Azufres presented in Cathelineau (1988) does not indicate the extent to which Ca, Na, and K are present.

Several workers have suggested modifications to Eq. 12, purely on empirical grounds, to take into account the variation in Fe/(Fe + Mg) in chlorite. Kranidiotis and MacLean (1987) modified the Cathelineau and Nieva (1985) expression by calculating a corrected Al^{IV} value (Al_C^{IV}) as follows:

$$Al_C^{IV} = Al^{IV} + 0.7(Fe/[Fe + Mg]), \quad (13)$$

from which the temperature, T (in °C), is then computed according to:

$$T = 106\ Al_C^{IV} + 18. \quad (14)$$

Kranidiotis and MacLean (1987) argued that their function is applicable to situations where chlorite grows in an "Al-saturated environment," i.e., in the presence of other aluminous minerals.

E. C. Jowett (personal communication) queried the validity of Kranidiotis and MacLean's (1987) modification as it was not based on compositions of chlorites which were known to have grown at the same temperature. Jowett (1991) suggested a similar type of correction, derived from an isothermal Fe/(Fe + Mg) normalization based on Salton Sea and Los Azufres chlorite compositions:

$$Al_C^{IV} = Al^{IV} + 0.1(Fe/[Fe + Mg]), \quad (15)$$

$$T = 319\,Al_C^{IV} - 69. \quad (16)$$

Jowett (1991) claimed that this Fe-Mg-modified geothermometer is applicable to a variety of systems in the range 150° to 325°C for chlorites with Fe/(Fe + Mg) values < 0.6.

A STEP BEYOND THE EMPIRICAL APPROACH

Although the simplicity of the empirical geothermometers makes them attractive, it will be shown in the discussion below that they are not particularly accurate over the temperature range from 25° to 350°C. The previous remarks on the effects of fluid and/or rock composition upon chlorite composition illustrate, in a qualitative way, that the extent of the Tschermak substitution in the general case must be controlled by other factors in addition to temperature. This argument may be partially quantified by considering chlorite in a simplified four-component system consisting of SiO_2, Al_2O_3, RO, and H_2O, where R is equivalent to either Mg or Fe^{2+}. The three molecular components of chlorite in this system may be taken to be $R_6Si_4O_{10}(OH)_8$, $R_5AlSi_3AlO_{10}(OH)_8$ and $Al_4\square_2Si_4O_{10}(OH)_8$ (after Table 1).

Assuming that the effects of pressure can be ignored, there are five constraints required to uniquely define this system. The five variables may be expressed as T, aH_4SiO_4, $aAl^{3+}/(aH^+)^3$, $aR^{2+}/(aH^+)^2$ and aH_2O.

If chlorite grows in contact with an aqueous phase and in equilibrium with quartz, which may be assumed to buffer the activity of SiO_2, then there are two degrees of freedom. Hence, the Tschermak substitution must be a function of two variables, say temperature and $aAl^{3+}/(aH^+)^3$, not just temperature. The relationship between temperature and $aAl^{3+}/(aH^+)^3$ may be described by a reaction between fluid and mineral as follows:

$$6\,R_5AlSi_3AlO_{10}(OH)_8 + 36\,H^+_{aq} + 2\,SiO_2 \leftrightarrows 5\,R_6Si_4O_{10}(OH)_8 + 12\,Al^{3+}_{aq} + 22\,H_2O_{(l)}. \quad (17)$$

From the law of mass action for reaction 17, we obtain:

$$\frac{a(R_6Si_4O_{10}(OH)_8)^5}{a(R_5AlSi_3AlO_{10}(OH)_8)^6} = \frac{K_{17}}{aAl^{3+}_{aq}/(aH^+_{aq})^3}, \quad (18)$$

which expresses the extent of the Tschermak exchange as a function of the ratio of the activities of the aluminum to hydrogen ions in solution, $aAl^{3+}_{aq}/(aH^+_{aq})^3$, as well as K_{17}, the equilibrium constant, which is a function of temperature and pressure. Clearly, one approach to utilizing the extent of the Tschermak exchange in chlorite as a geothermometer necessitates the presence of a mineral or mineral assemblage that buffers the variable $aAl^{3+}_{aq}/(aH^+_{aq})^3$.

An alternative approach adopted by Walshe (1986) is to make use of the di-tri substitution in the octahedral site of chlorite (exchange Reaction 5, Table 1) to monitor the value of the ratio $aAl^{3+}_{aq}/(aH^+_{aq})^3$ via the reaction:

$$Al_4\square_2Si_4O_{10}(OH)_8 + 12\,H^+_{aq} \leftrightarrows 4\,Al^{3+}_{aq} + 4\,SiO_2 + 10\,H_2O_{(l)}. \quad (19)$$

Combining Eqs. 17 and 19 leads to the geothermometer:

$$6\,R_5AlSi_3AlO_{10}(OH)_8 + 8\,H_2O_{(l)} + 14\,SiO_2 \leftrightarrows 5\,R_6Si_4O_{10}(OH)_8 + 3\,Al_4\square_2Si_4O_{10}(OH)_8, \quad (20)$$

which is independent of the $aAl^{3+}_{aq}/(aH^+_{aq})^3$ ratio. The advantage of this geothermometer is obvious in that it suffices that quartz and chlorite coexist in equilibrium at any given pressure.

THE SIX-COMPONENT THERMODYNAMIC MODEL AND QUARTZ-CHLORITE GEOTHERMOMETRY

A limitation to the use of Eq. 20 as a geothermometer is that the size of the octahedral vacancy created by the di-tri substitution is a function of the assumed amount of ferric iron in the mineral, or the redox state of the environment in which chlorite grew. Ferric iron may substitute into the chlorite structure for either aluminum or ferrous iron (Exchanges 4 and 6, Table 1). The conversion of assumed ferrous iron to the ferric iron that substituted into the structure via Exchange 4 (Table 1) involves an adjustment to the number of oxygen atoms in the structural formula. For every mole of Fe^{2+} converted to Fe^{3+}, a half-mole of oxygen is added to the structure, as indicated by the iron conservative reaction:

$$FeO + 0.5\,O \leftrightarrows FeO_{1.5}. \quad (21)$$

This necessitates an adjustment to the number of cations per 14 oxygen atoms (based on an anhydrous half-cell formula) of 14/(14 + x/2), where x is the number of ferrous atoms converted to ferric atoms via this exchange (Walshe, 1986). Therefore, increasing the assumed ferric iron via Exchange 4 (Table 1) reduces the number of cations and increases the size of the vacancy. Thus, as noted above, a good chlorite analysis in which the cation total exceeds 10 when the assumption of 14 oxygen atoms per half-cell is made has the potential to yield information on the *minimum* extent of sub-

https://doi.org/10.1346/CCMN.1993.0410210 Published online by Cambridge University Press

stitution of Fe^{3+} for Al^{VI}. On the other hand, the number of oxygen atoms in the structure is unaffected by the conversion of ferrous iron to ferric iron to take account of the latter substitution (Exchange 6), in which charge is balanced by a loss of hydrogen from the structure:

$$Fe(OH)_2 \leftrightarrows FeO(OH) + H. \quad (22)$$

Walshe (1986) attempted to resolve this problem by considering a six-component chlorite model. In this expanded system (Table 1), there are two independent geothermometers/geobarometers, which in theory could be utilized to determine the temperature and pressure of formation of a fully analyzed chlorite coexisting with quartz:

$$6\,Mg_5AlSi_3AlO_{10}(OH)_8 + 8\,H_2O_{(l)} + 14\,SiO_2 \leftrightarrows 5\,Mg_6Si_4O_{10}(OH)_8 + 3\,Al_4\square_2Si_4O_{10}(OH)_8, \quad (23)$$

which corresponds, in terms of the molecular components of Table 1 (denoted C1, C2, etc.), to:

$$6C2 + 8\,H_2O_{(l)} + 14\,SiO_2 \leftrightarrows 5C1 + 3C5, \quad (24)$$

and,

$$42\,Mg_5AlSi_3AlO_{10}(OH) + 30\,Fe_5^{2+}Si_3Fe^{3+}O_{10}(OH)_8 + 18\,Fe_5^{2+}AlSi_3AlO_{10}(OH)_8 + 50\,SiO_2 \leftrightarrows 60\,Fe_5^{2+}Fe^{3+}AlSi_3AlO_{11}(OH)_7 + 35\,Mg_6Si_4O_{10}(OH)_8 + 10\,H_2O_{(l)}, \quad (25)$$

which corresponds to:

$$42C2 + 30C4 + 18C3 + 50\,SiO_2 \leftrightarrows 60C6 + 35\,Cl + 10\,H_2O_{(l)}. \quad (26)$$

As the ferric iron and water contents of chlorites are (generally) unknown, Eqs. 23 and 25 can be combined with a statement of the Gibbs-Duhem equation for chlorite to provide three constraints to solve three unknowns: T, X4 (or the equivalent variable x) and X6. This procedure also allows calculation of the redox conditions (fO_2) of chlorite formation in addition to the variables $a\mathrm{Al}^{3+}/(a\mathrm{H}^+)^3$, $a\mathrm{Mg}^{2+}/(a\mathrm{H}^+)^2$ and $a\mathrm{Fe}^{2+}/(a\mathrm{H}^+)^2$.

The six-component chlorite model predicts a curvilinear relationship between temperature and Si^{IV}, as illustrated in Kavalieris *et al.* (1990, Figure 14), and only minimal variation in the parameter $a\mathrm{Al}^{3+}/(a\mathrm{H}^+)^3$. Hence, in practice, this geothermometer is only valid over a narrow range of $a\mathrm{Al}^{3+}/(a\mathrm{H}^+)^3$ at any temperature (see discussion).

As part of a reassessment of quartz-chlorite geothermometry, Walshe and Harrold (in prep.) address the difficulties highlighted here, and develop some semiempirical geothermometers based on the Tschermak and di-tri substitutions in chlorite, consistent with the theoretical constraints discussed above.

CHLORITE-CARBONATE EQUILIBRIA AND GEOTHERMOMETRY

The importance of clay-carbonate reactions at relatively low temperatures was first recognized by Zen (1959). Since then, clay-carbonate assemblages have been documented in geothermal systems (Muffler and White, 1969; McDowell and Paces, 1985) and in diagenetic settings (Hutcheon *et al.*, 1980; Hutcheon, 1990). Hutcheon *et al.* (1980) described how clay-carbonate reactions may buffer the CO_2 composition of the liquid phase to increasing values of dissolved CO_2 with increasing temperature and progress of clay-carbonate reactions. They suggested that the intersection between clay-carbonate reactions, traced on a temperature *vs* XCO_2 diagram, and the miscibility surface between CO_2 and H_2O could be used as an indicator of the maximum temperature at which chlorite, kaolinite, and a carbonate can coexist in the presence of a liquid phase.

Hutcheon *et al.* (1980) obtained the thermodynamic properties of all the solids and water from the one-phase liquid region (i.e., at CO_2 concentrations lower than saturation) and the properties of CO_2 in the vapor phase (i.e., at CO_2 concentrations higher than saturation). This was done in order to avoid the impossible task of calculating the distribution of carbonate species in an aqueous solution without specifying its pH. The availability of thermodynamic data for CO_2 as an aqueous species in the one-phase liquid region (Johnson *et al.*, 1992) and Henry's law data for the equilibrium between $CO_{2(aq)}$ and $CO_{2(v)}$ (Barta and Bradley, 1985) make possible the calculation of the stability of clay-carbonate reactions in the one-phase liquid region. This allows the effect of pressure and salinity on these reactions to be evaluated explicitly and permits re-evaluation of the potential for the clay-carbonate method to be used as a geothermometer. In addition, the new calculations provide a more rigorous means of examining the controls of chlorite stability in H_2O-CO_2-NaCl fluids in a general sense.

The paths of equilibria within the one-phase liquid field, such as those given below:

$$5\,CaMg(CO_3)_2 + Al_2Si_2O_5(OH)_4 + SiO_2 + 2\,H_2O \leftrightarrows Mg_5AlSi_3AlO_{10}(OH)_8 + 5\,CaCO_3 + 5\,CO_2, \quad (27)$$

$$5\,FeCO_3 + Al_2Si_2O_5(OH)_4 + SiO_2 + 2\,H_2O \leftrightarrows Fe_5AlSi_3AlO_{10}(OH)_8 + 5\,CO_2, \quad (28)$$

can be calculated as a function of temperature and define paths of CO_2 concentration required in the liquid at equilibrium. If chlorite is assumed to form near equilibrium with the coexisting fluid at any given tem-

https://doi.org/10.1346/CCMN.1993.0410210 Published online by Cambridge University Press

Table 2. Composition of selected chlorites.

Sample	WB-1	ON-1	ON-5	VF-4	SS-2	SS-12	LA-1	LA-9	BO-1
Depth (m)	surface	2852	4357	4959	439	1064	—	—	1125
T (°C)[1]	25	110	155	140	190	322	130	310	290
P (MPa)[2]	—	40	42	83	—	—	—	—	—
Chemical composition (wt. %)[3]									
SiO_2	33.63	28.49	24.75	23.71	27.65	26.79	35.26	28.56	23.03
Al_2O_3	12.24	20.31	23.53	22.04	18.15	18.98	15.61	18.73	20.71
Fe_2O_3	0.00	0.00	0.00	0.00	0.00	0.00	0.00	0.00	0.00
FeO	26.02	32.73	35.77	33.07	31.30	24.23	13.35	20.54	37.16
MnO	0.30	—	—	0.28	0.55	0.68	—	0.23	3.03
MgO	15.36	6.48	3.95	4.84	10.36	17.34	23.80	19.96	3.63
CaO	0.53	—	—	0.12	—	—	—	—	—
Na_2O	—	—	—	0.26	—	—	—	—	—
TiO_2	—	—	—	0.38	—	—	—	—	—
NiO	0.17	—	—	—	—	—	—	—	—
K_2O	—	—	—	0.08	—	—	—	—	—
Total	88.25	88.01	88.00	84.78	88.01	88.02	88.02	88.02	87.56
Structural formulae (half-cell)[4]									
Si^{IV}	3.50	3.07	2.73	2.71	2.99	2.80	3.41	2.91	2.65
Al^{IV}	0.50	0.93	1.27	1.29	1.01	1.20	0.59	1.09	1.35
Al^{VI}	1.00	1.65	1.79	1.68	1.30	1.14	1.19	1.16	1.46
Fe^{VI}	2.26	2.95	3.30	3.16	2.83	2.12	1.08	1.75	3.57
Mg^{VI}	2.38	1.04	0.65	0.82	1.67	2.70	3.43	3.03	0.62
Mn^{VI}	0.03	0.00	0.00	0.03	0.05	0.06	0.00	0.02	0.30
Σ^{VI}	5.67	5.64	5.74	5.69	5.85	6.03	5.70	5.96	5.95
Fe/(Fe + Mg) and Fe/Mg									
Fe/(Fe + Mg)	0.49	0.74	0.84	0.79	0.63	0.44	0.24	0.37	0.85
Fe/Mg	0.95	2.84	5.08	3.85	1.70	0.78	0.31	0.58	5.76
End-member proportions									
"Al-chl"	0.14	0.24	0.28	0.27	0.20	0.20	0.16	0.19	0.25
"Fe-chl"	0.42	0.56	0.60	0.58	0.50	0.35	0.20	0.30	0.64
"Mg-chl"	0.44	0.20	0.12	0.15	0.30	0.45	0.64	0.51	0.11

[1] Temperatures (T) are from Jahren and Aagaard (1989, 1992) for offshore Norway (ON); Hutcheon (1990, Figure 2) for Venture Field (VF); McDowell and Elders (1980, Table 3) for Salton Sea (SS); Cathelineau (1988, Table 1) modified after Cathelineau and Nieva (1985, Table 3) for Los Azufres (LA); and Lonker *et al.* (1990, Table 3) for Broadlands-Ohaaki (BO); temperature for weathered basalt (WB) estimated (Walshe, unpublished data; Eggleton *et al.*, 1987).

[2] Pressure (P) is an approximation; references as for temperature where applicable.

[3] Chemical compositions (oxides) are from R. A. Eggleton (personal communication) for WB; Hutcheon (1990, Table 1) for VF; and Lonker *et al.* (1990, Table 3) for BO. All other compositions are back-calculated from structural formulae, based on ≈88% total anhydrous oxide and assuming 14 oxygen atoms per half-cell and no ferric iron.

[4] Structural formulae from Jahren and Aagaard (1992) for ON; Walshe (1986, Table 4) modified after McDowell and Elders (1980, Table 3) assuming 14 oxygen atoms for SS; Cathelineau (1988, Table 1) for LA; and Lonker *et al.* (1990, Table 3) for BO; all other structural formulae are calculated from chemical compositions, assuming 14 oxygen atoms per half-cell and no ferric iron.

perature and the clinochlore and daphnite reactions (Eqs. 27 and 28, respectively) are correctly calibrated by thermodynamic data and chemical analyses of the relevant phases, the clinochlore and daphnite reaction curves should intersect the CO_2-H_2O miscibility surface at that same temperature on a temperature versus XCO_2 graph.

In theory, if a chlorite-carbonate assemblage coexists with a CO_2-saturated fluid, the temperature of intersection of Reactions 27 or 28 with the CO_2-H_2O miscibility surface and the temperature obtained from Walshe's (1986) method should be coincident, since both approaches rely on thermodynamic principles and properties to decipher the chlorite composition-temperature relationship. In practice, however, differences in temperatures estimated by these two methods are observed (see below), and likely result from: 1) differences in calibration of thermodynamic properties for the minerals involved; and 2) differences in methods of obtaining the activity of chlorite end-member components from chemical analyses. In particular, the estimate of Gibbs free energy for daphnite ($Fe_5AlSi_3AlO_{10}(OH)_8$) is probably not as reliable as that for clinochlore ($Mg_5AlSi_3AlO_{10}(OH)_8$). In the following calculations, the free energy of daphnite is taken from Walshe (1986); that of clinochlore is taken from SUPCRT92 (Johnson *et al.*, 1992).

Chlorite analyses from Table 2 that are amenable to the present method of calculation by virtue of having grown in contact with a liquid phase, i.e., those ob-

tained from sedimentary basins (VF-4, ON-1 and ON-5), were used to estimate temperatures. The calculation of the position of Reactions 27 and 28 was completed as follows. The standard state for minerals, aqueous species, including $CO_{2(aq)}$, and liquid water was considered to be the pure component at the temperature and pressure of interest. The standard state for $CO_{2(v)}$ was taken to be the pure component at one bar and at the temperature of interest. The equilibrium constants for Reactions 27 and 28 were calculated using SUPCRT92 (Johnson *et al.*, 1992). Assuming that kaolinite, dolomite, and quartz can be considered to be pure minerals and that liquid water up to 20 wt. % total salinity as NaCl has an activity close to unity, the equilibrium constant for Reaction 27 is given by:

$$\log K_{27} = 5 \log aCO_2^{aq} + 5 \log a_{Calcite}^{CaCO_3} + \log a_{Chlorite}^{Clinochlore}, \quad (29)$$

and the equilibrium constant for Reaction 28 is:

$$\log K_{28} = 5 \log aCO_2^{aq} - 5 \log a_{Siderite}^{FeCO_3} + \log a_{Chlorite}^{Daphnite}, \quad (30)$$

where $a_{Chlorite}^{Clinochlore}$, for instance, represents the activity of clinochlore in chlorite, and is calculated as the mole fraction of clinochlore in chlorite, according to:

$$a_{Chlorite}^{Clinochlore} = \frac{Mg^{VI}}{\Sigma^{VI} - 1} \cdot Al^{VI} \cdot Al^{IV} \cdot \frac{Si^{IV}}{3}. \quad (31)$$

By calculating the mole fraction of clinochlore in chlorite as shown in Eq. 31, that of daphnite in chlorite in a similar fashion, and those of $CaCO_3$ and $FeCO_3$ in calcite and siderite, respectively (chemical analyses in Table 2 from Hutcheon, 1990, for Sample VF-4, and Jahren and Aagaard, 1992, for samples ON-1 and ON-5), the activity of CO_2 in the aqueous phase can be calculated for each equilibrium. The equations of Barta and Bradley (1985) are used to obtain the equilibrium constant for the reaction:

$$CO_2^{aqueous} \leftrightarrows CO_2^{vapor}, \quad (32)$$

according to:

$$\log K_{32} = \log fCO_2^{vapor} - \log aCO_2^{aqueous}, \quad (33)$$

and to obtain the fugacity of CO_2^{vapor} from the activity of $CO_2^{aqueous}$ at 0, 6 and 20 wt. % NaCl. Using fugacity coefficients for CO_2, the partial pressure and mole fraction of CO_2 in equilibrium with Reactions 27 and 28 can be calculated. Fugacity coefficients for CO_2 were interpolated from the compilation of Angus *et al.* (1976) below 1000 bars, or calculated from free energies tabulated by Bottinga and Richet (1981) using the equation:

$$\mu_{CO_2} = \mu^{\circ}_{CO_2} + RT \ln fCO_2. \quad (34)$$

To obtain the position of the intersections between Reactions 27 and 28 and the miscibility surface, the solubility of CO_2 in an aqueous phase with 0, 6 and 20 wt. % NaCl (or 0, 1.1 and 4.3 m NaCl) was interpolated in terms of XCO_2 at the relevant pressure and salinity, using the data of Sourirajan and Kennedy (1962), Takenouchi and Kennedy (1965), and Bowers and Helgeson (1983). The position of the clinochlore reaction equilibrium (Eqs. 27 and 29) and the CO_2 solubility surfaces for these three samples (VF-4, ON-1 and ON-5) are shown in Figure 3, and the temperatures corresponding to their intersections are found to be very sensitive to the salinity of the aqueous phase. Calculations for ON-1 and ON-5 were done at 40 and 42 Mpa, respectively (Jahren and Aagaard, 1989). The range of salinity for porewaters in the North Sea sedimentary basin, offshore Norway, is approximately 2 to 30 equivalent wt. % NaCl (Egeberg and Aagaard, 1989). Without more specific information on the salinity at the depth of each sample, obtaining exact temperature estimates is not possible. Assuming an approximate salinity of 6 wt. % gives temperatures of 80°C for both samples (Figure 3), lower than the 100°C and 155°C reported by Jahren and Aagaard (1992) for ON-1 and ON-5, respectively. Hutcheon (1990) reported that pressure in the Venture Field increases rapidly from approximately 40 MPa just above the over-pressured zone to about 80 MPa within it. Consequently, calculations were done for sample VF-4 at both pressures (Figure 3). Analyses of fluids from drill stem tests in the Venture Field indicate that the total salinity (expressed as equivalent NaCl) is in the range of 20 to 25 wt. %. At 80 MPa and 20 wt. % NaCl, the position of the reaction-miscibility intersection suggests a temperature for chlorite formation of approximately 80°C (Figure 3), a value lower than the 140°C present-day temperature reported for the depth of this sample (Hutcheon, 1990).

These low calculated temperatures could result from the fact that the position of the reaction-miscibility intersection is sensitive to the thermodynamic properties of chlorite, the activity-composition model used for individual chlorite compositions, the calculation of aCO_2 from fCO_2, and the fluid salinity. All these factors probably introduce substantial errors and may render this method too sensitive for practical application as a geothermometer. However, the calculations show that clay-carbonate reactions are realistic sources of CO_2 during the course of burial diagenesis.

Alternatively, the low temperatures calculated using the above method may reflect the time required during diagenesis for individual chlorite grains to grow to a size suitable for probe analysis. Based on TEM analyses and crystal growth calculations, Jahren (1991) suggested that individual chlorite grains may grow over a temperature range of 50°C or more during progressive burial. This suggestion is consistent with the buffering of the CO_2 concentration in the fluid by clay-carbonate

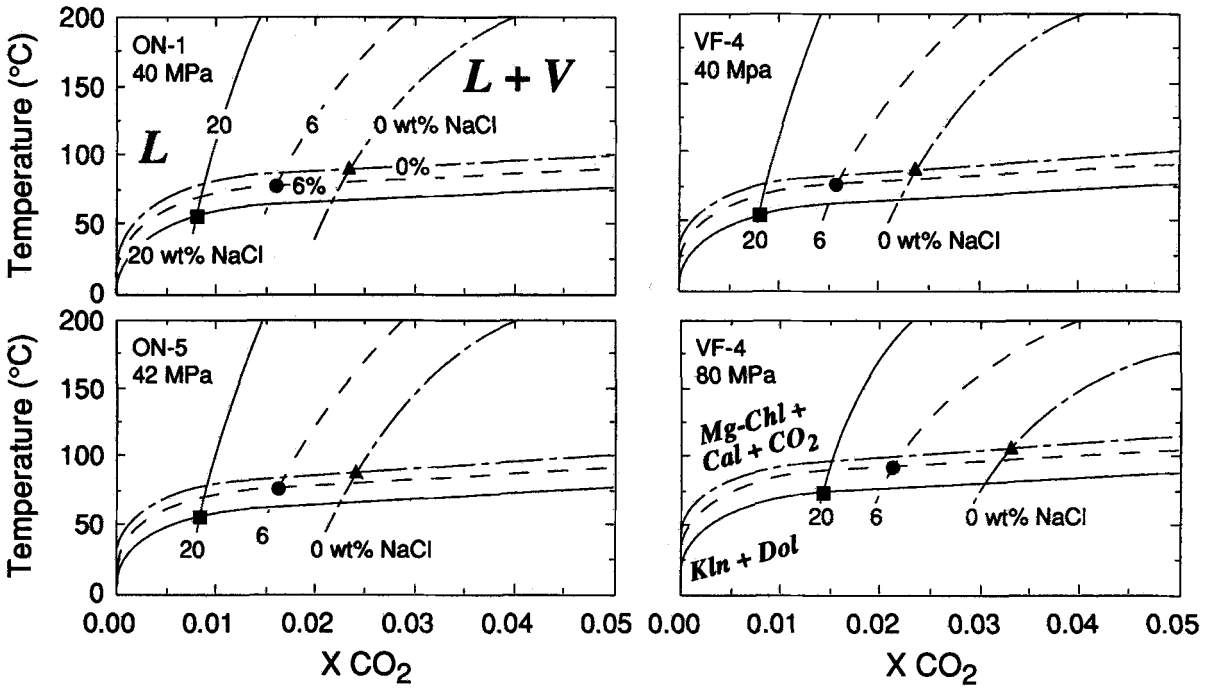

Figure 3. Temperature *vs* XCO_2 plots showing the position of the kaolinite + dolomite ⇆ chlorite + calcite + CO_2 reaction curves (Eq. 27 in text), as well as the position of the H_2O-CO_2 miscibility surfaces, which separate the one-phase liquid region (L) from the two-phase liquid plus vapor region (L + V), for three different salinities. The reaction curves delimit the stability fields of kaolinite + dolomite below them, and chlorite + calcite + CO_2 above them (the reaction takes place to the left of, or on, the appropriate miscibility curve, i.e., in contact with a liquid phase). The diagrams on the left are for chlorite analyses ON-1 (top) and ON-5 (bottom), whereas the diagrams on the right are both for sample VF-4 of Table 2. Pore-fluid pressure used for the calculations are 40 MPa for ON-1, 42 MPa for ON-5, and both 40 and 80 MPa for VF-4. The position of the reaction-miscibility intersections are shown for various salinities (0, 6 and 20 wt. % equivalent NaCl).

reactions. Indeed, with each increment of reaction as temperature increases during burial, a new, higher CO_2 concentration will be established. At each stage of burial only a small amount of chlorite will grow. It is possible, therefore, that the composition of chlorite grains varies during growth and that compositions obtained by electron microprobe are averages of many fine zones. These zones may reflect the buffering process that took place during the progress of clay-carbonate reactions as burial depth increased.

To examine the consequences of buffering CO_2 in this way, the procedure outlined above was applied to the calculation, using a forward modeling approach, of the path of chlorite-carbonate equilibria with varying temperature, pressure and salinity. To account for the range of physical conditions in most sedimentary basins, temperature-pressure trajectories were used based on a low geotherm (20°C/km) and a high geotherm (30°C/km), with pressure gradients ranging from hydrostatic (10 MPa/km) to lithostatic (22 MPa/km). Salinities in the range 0 to 20 wt. % NaCl were also used in this exercise.

Analyses of chlorites and carbonates from the Venture Field (Hutcheon, 1990) were used for purposes of these calculations. One of the chosen samples is from well B-13 at 4951 m depth, corresponding to a measured temperature (corrected from drilling data) of approximately 138°C; and a second sample is from well J-16 at 5168 m depth, corresponding to a measured (corrected) temperature of approximately 142°C. The activity of the thermodynamic components daphnite and clinochlore as end-members in chlorite, and of $FeCO_3$ and $CaCO_3$ in siderite (J-16) and calcite (B-13), respectively, were considered to be equal to the mole fractions, as detailed earlier.

Calculations for the range of chlorite compositions in Table 2 show that the daphnite reaction (Eq. 28) does not intersect the CO_2 miscibility surface for any of the chlorite compositions at any temperature and pressure (using 20°C/km or 30°C/km geotherms and hydrostatic or lithostatic pressure gradients). This probably reflects the uncertainty in the free energy data for daphnite. However, the clinochlore reaction (Eq. 27) intersects the miscibility surface for all ranges of temperature, pressure and salinity. Calculations for the sample from well J-16 are presented in detail here (Figure 4). The calculated position of the intersections (Figure 4) shows that the clay-carbonate reaction intersects the miscibility surface at lower temperatures as salinity increases and/or pressure decreases. This reflects the

https://doi.org/10.1346/CCMN.1993.0410210 Published online by Cambridge University Press

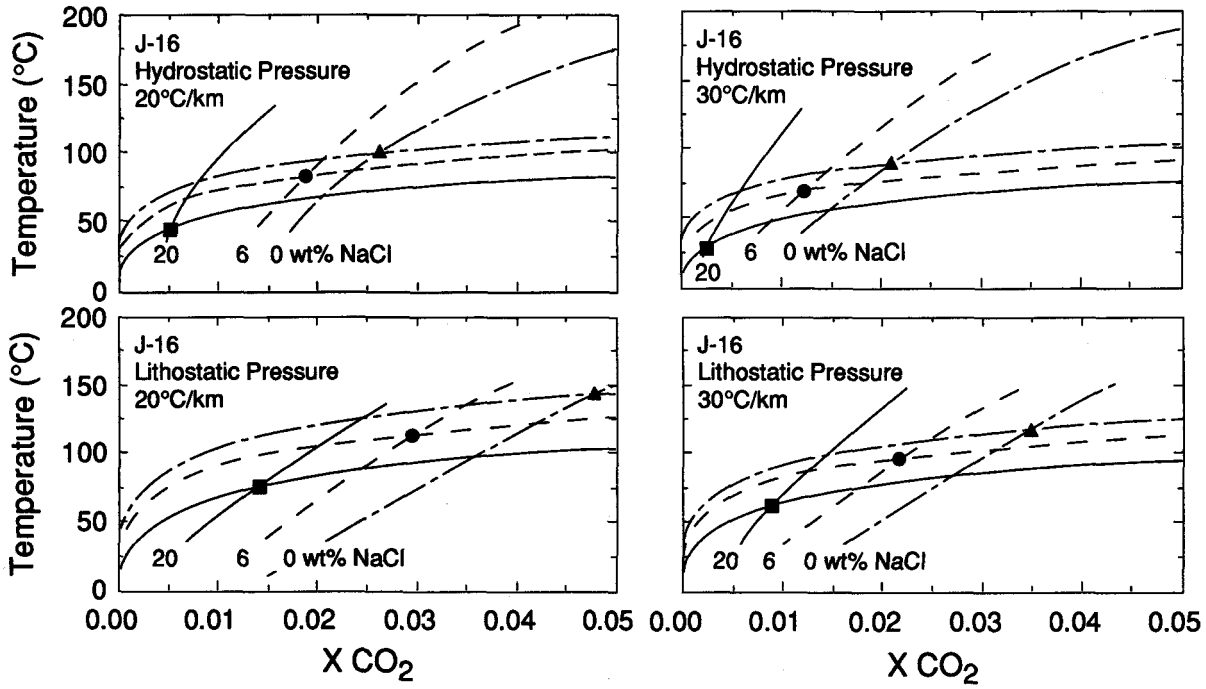

Figure 4. Same diagram as in Figure 3, except that here the evolution along indicated temperature and pressure gradients is illustrated, rather than a static situation as in Figure 3. Chlorite composition used here is from well J-16 (5168 m depth) in the Venture Field (Hutcheon, 1990). Note that the temperature corresponding to the reaction-miscibility intersection decreases as salinity increases, increases as the pressure gradient increases (compare top and bottom figure on each side), and decreases as the geotherm increases (compare top left and right, or bottom left and right figures).

increase in CO_2 solubility in the liquid phase as salinity decreases and pressure increases. The effect of variation in chlorite composition on the position of the reaction-miscibility intersection is minor, suggesting that the composition of chlorite, at least in terms of the activity of daphnite and clinochlore end-members, is not an effective temperature indicator when used with the CO_2 miscibility surface geothermometry method. Greater temperature variations would probably be observed by considering the possible errors in the free energy of the end-members or by selecting alternative methods of calculating the activity-composition relationship of end-member components than can be introduced by changing the compositions themselves.

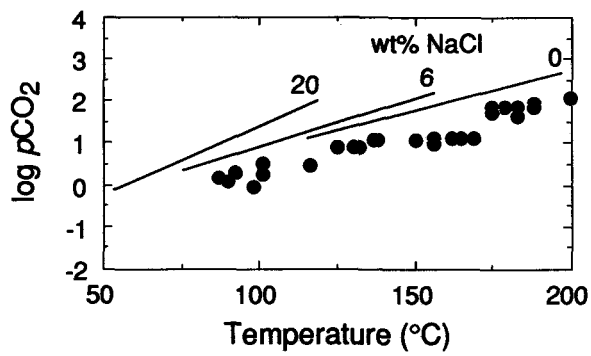

Figure 5. Data from the Texas Gulf Coast (solid circles) given in Smith and Ehrenberg (1989) plotted in a log pCO_2 versus temperature diagram. The lines tie together the intersections between the chlorite-carbonate reaction (Eq. 27) and the H_2O-CO_2 miscibility surface for three different values of pore-fluid salinities, as indicated in wt. % equivalent NaCl. The general agreement in slope and absolute values between the data points and the modeling curves suggests that the chlorite-carbonate reaction considered may in part control pCO_2 in sedimentary basins.

Hutcheon (1990) suggested that the trend of relatively linear log pCO_2 values as a function of temperature, reported for the North Sea and Texas Gulf Coast by Smith and Ehrenberg (1989) may result from the intersection of clay-carbonate reactions with the CO_2 miscibility surface as pressure and temperature increase during burial. The calculation method outlined above offers a test of this suggestion. Data from the Texas Gulf Coast (Smith and Ehrenberg, 1989) are plotted in a log pCO_2 versus temperature diagram (Figure 5), and so are lines showing the position of intersections between the reaction of Eq. 27 and the CO_2 miscibility surface as calculated for VF-4, using hydrostatic and lithostatic pressure gradients and geotherms of 20 and 30°C/km. The traces of the intersections define a set of three nearly straight lines in log pCO_2-temperature space, one for each of the three salinity values used (0, 6 and 20 wt. % NaCl). In general, the position of the intersection points is relatively insensitive to chlorite composition, at least in the range

https://doi.org/10.1346/CCMN.1993.0410210 Published online by Cambridge University Press

Table 3. Comparison of coexisting assemblages and geothermometer results.

Sample	WB-1	ON-1	ON-5	VF-4	SS-2	SS-12	LA-1	LA-9	BO-1
Fe/(Fe + Mg)	0.49	0.74	0.84	0.79	0.63	0.44	0.24	0.37	0.85
Al^{IV}	0.50	0.93	1.27	1.29	1.01	1.20	0.59	1.09	1.35
					Coexisting assemblages[1]				
	Pl-Px-14Å Chl after Ol	Qtz-sChl-Kln	Qtz-Ill-Kln-Chl	Qtz-Ab-Ill-?Ank-Kln-Chl	Qtz-Ser-Kfs-Ank-Cal-Dol-Ill/Sm-Pl-Hem-Chl	Qtz-Ms-Ank-Cal-Ab-Pl-Ill-Py-Chl	Qtz-Ill-Ab-Cal-Py-Chl	Qtz-Ill-Hem-Chl	Qtz-Ill-Kfs-Chl
					Temperatures (°C)[2]				
"Actual" *T*	25	110	155	140	190	322	130	310	290
C88	99	238	347	353	263	323	128	289	373
KM87	107	171	215	214	172	177	98	161	224
J91	106	251	363	368	273	327	127	290	389
W86	36	146	252	254	171	263	78	213	303
H90	—	80	80	80	—	—	—	—	—

[1] Rock-forming minerals: Ab, albite; Ank, ankerite; Cal, calcite; Chl, chlorite; Dol, dolomite; Hem, hematite; Ill, illite; Ill/Sm, interstratified illite/smectite; Kfs, K-feldspar; Kln, kaolinite; Ms, muscovite; Ol, olivine; Pl, plagioclase; Px, pyroxene; Py, pyrite; Qtz, quartz; sChl, swelling chlorite; Ser, sericite; see Table 2 for references.

[2] Geothermometers used: C88, Cathelineau (1988); KM87, Kranidiotis and MacLean (1987); J91, Jowett (1991), strictly speaking only applicable to chlorites with Fe/(Fe + Mg) < 0.6; W86, Walshe (1986); and H90, Hutcheon (1990) (see Table 2 for data source).

of chlorite compositions encountered in the Venture Field (Hutcheon, 1990).

The calculations done here (Figure 5) are based on the assumption that the proportion of clinochlore in chlorite is not a function of temperature. In natural settings spanning a more complete temperature-pressure spectrum, chlorites are expected to exhibit a greater compositional variation than shown in the Venture Field. The general tendency for chlorites to be more iron-rich at low temperature and to increase in Mg-content with increasing temperature requires that the intersection points be defined by chlorites that are increasingly magnesian as temperature rises during burial. The increase in Mg-content with temperature would increase the activity of the clinochlore end-member, thus decreasing the stability field of chlorite and causing the intersection points to shift to relatively higher temperatures as temperature increases during chlorite growth as burial proceeds. This effect of changing chlorite composition during burial would affect the slope of the lines in Figure 5 so that they cannot be linearly extrapolated over a wide temperature range but rather should display a curved shape (decreasing slope as temperature increases).

Other clay-carbonate reactions can be considered in order to explain the observed pCO_2-temperature trends, and Smith and Ehrenberg (1989) suggested that illite, K-feldspar and kaolinite, among other silicates, may react with calcite to produce the trends observed in the Gulf Coast and in the North Sea. It is possible that explicit calculation of the intersection of these reactions with the miscibility surface will provide a better correspondence between observed and calculated pCO_2 values. Hutcheon *et al.* (1993) have evaluated the pH buffer capacity of various silicate and aqueous species, and concluded that silicate-carbonate assemblages are capable of mediating pH, and thus pCO_2, in a burial diagenetic assemblage.

DISCUSSION: COMPARISON OF CHLORITE GEOTHERMOMETERS

Presently, structural chlorite geothermometry (polytype geothermometry) is largely qualitative and poorly understood. This is reflected by the fact that the I*b* ($\beta = 90°$) to II*b* transition temperature appears to fluctuate from 50°C (Walker, 1989) to 200°C (Hayes, 1970). Weaver *et al.* (1984) even suggested that polytype I*a* could persist to temperatures of the order of 300°C. The polytype transition in chlorite appears to also depend on factors other than temperature (e.g., grain size of the hosting medium, pressure, time, etc.) that need to be systematically investigated. For these reasons, and because chlorite polytype is still rarely reported in the literature, the remainder of the present discussion will focus on the composition (chemical) chlorite geothermometers.

In order to illustrate the effects of bulk rock composition and formation temperature on chlorite composition, analyses of chlorites from the regolith, sedimentary basins, and geothermal fields have been selected for which temperature, pressure, and/or depth information was available (Tables 2 and 3). These selected chlorites (Table 2) are from: 1) a surficial weathering profile (WB), New South Wales (Tertiary, basalt; Eggleton *et al.*, 1987, R. A. Eggleton, personal communication); 2) offshore Norway (ON), North Sea Basin (Jurassic, feldspathic sandstones; see Jahren and Aagaard, 1989 and 1992); 3) the Venture Field (VF),

https://doi.org/10.1346/CCMN.1993.0410210 Published online by Cambridge University Press

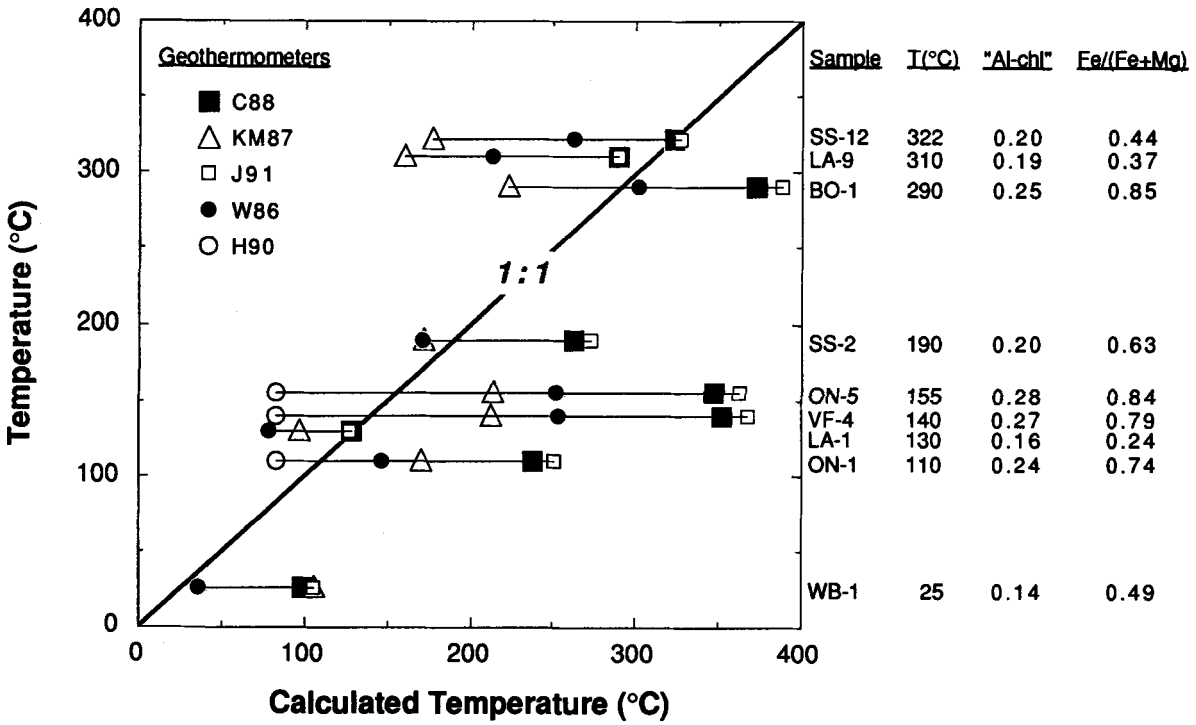

Figure 6. Comparison of performance of various chlorite geothermometers in terms of calculated temperature plotted against measured temperature of chlorite formation. See text for detailed discussion. Geothermometers: C88, Cathelineau (1988); KM87, Kranidiotis and MacLean (1987); J91, Jowett (1991); W86, Walshe (1986); and H90, Hutcheon (1990).

Scotian Shelf (Lower Cretaceous, quartzose to feldspathic sandstones; see Hutcheon, 1990); 4) the Salton Sea geothermal field (SS), California (hydrothermally altered recent feldspathic sandstones and feldspathic argillaceous sandstones: McDowell and Elders, 1980); 5) the Los Azufres geothermal field (LA), Mexico (hydrothermally altered recent andesites: see Cathelineau and Nieva, 1985; Cathelineau, 1988; and Cathelineau and Izquierdo, 1988); and 6) the Broadlands-Ohaaki geothermal field (BO), New Zealand (hydrothermally altered Quaternary quartzitic volcanic rocks and sedimentary rocks: see Lonker *et al.*, 1990). The chlorites selected for this comparison cover a broad range of compositions, coexist with a variety of mineral assemblages, and formed at temperatures ranging from 25° to 322°C.

The various compositional chlorite geothermometers discussed in this paper were applied to this selection of chlorite analyses. Results are shown in Table 3 and illustrated in Figure 6. In the following discussion, it will be assumed that the formation temperatures reported in the various studies from which the chlorite analyses were taken are correct. In most cases, present-day temperatures at the level of sampling are assumed to be representative of those under which chlorite grew or re-equilibrated. The study of Velde and Medhioub (1988) shows indeed that sedimentary chlorites are likely to continuously re-equilibrate under conditions of progressive burial.

Intersections of clay-carbonate reactions, within the one-phase liquid region, with the CO_2-H_2O miscibility surface are only possible if the fluid is not boiling (i.e., in sedimentary basins). Because the water in most geothermal systems is at, or near, boiling the calculation of clay-carbonate intersections with the miscibility surface is not feasible, and temperature estimates of chlorite formation in these settings is not possible using this method.

Both the Walshe (1986) and Hutcheon (1990) geothermometry methods use thermodynamic approaches; therefore, they should, in theory, yield similar estimates of the temperature of chlorite formation. Discrepancies existing between these two methods are likely to arise from the fact that slightly different thermodynamic properties were used and, more importantly, from different methods of estimating the activity-composition relationships. The empirical methods of Cathelineau (1988) and others, however, are not based on any thermodynamic foundation and are, therefore, not expected, in principle, to yield results similar to the two thermodynamic approaches. The empirical geothermometers rely on the variation in Si^{IV} (or Al^{IV}) with temperature. This value may be sensitive to changes in the activity of SiO_2 (or Al_2O_3) imposed by coexisting minerals via changes in activity of species dissolved in the fluid phase.

Figure 6 suggests that none of the available geothermometers satisfactorily predicts the formation

https://doi.org/10.1346/CCMN.1993.0410210 Published online by Cambridge University Press

temperature of chlorite over the range of composition and bulk rock mineralogy considered. Some calculations, especially near the mid-range temperatures (100°–200°C), overestimate the chlorite formation temperatures by up to 230°C, obviously an unsatisfactory result. In the high temperature range (>200°C), some of the geothermometers grossly underestimate the temperature of chlorite formation by up to 150°C.

The Si^{IV} content (or the related Al^{IV} content) of chlorite does not correlate well with formation temperature for the whole set of analyses considered here (Figure 7). This is an important point, because some empirical geothermometers directly link Al^{IV} (where Al^{IV} is taken to be equivalent to 4-Si^{IV}) to formation temperature (Cathelineau and Nieva, 1985; Cathelineau, 1988). The Cathelineau (1988) function overestimates chlorite formation temperatures by 75°–215°C for samples that were not used for its calibration. The seemingly good results of the Cathelineau (1988) (and the Jowett, 1991) geothermometer for the LA and SS samples should be considered keeping in mind that this function was calibrated with data from Los Azufres and Salton Sea.

Overall, the geothermometers based on the Cathelineau approach, that incorporate a correction for Fe/(Fe + Mg), do not perform much better than the original function. Particularly, the Jowett (1991) equation yields results very similar to the Cathelineau (1988) method (Figure 6), especially within the window of Fe/(Fe + Mg) values recommended by the author [Fe/(Fe + Mg) < 0.6; Jowett, 1991]. In fact, the Jowett (1991) correction tends to overestimate chlorite formation temperature even more than the original Cathelineau (1988) method for the selected chlorites.

In comparison, the function of Kranidiotis and MacLean (1987) yields calculated temperatures which may be either greater than or less than measured temperatures (Figure 6). The absolute differences between measured and these calculated temperatures vary between 20° and 150°C. Although high, these differences are smaller overall than the differences given by the functions of Cathelineau (1988) and Jowett (1991). For the ON, SS-2 and VF-4 samples, particularly, the Kranidiotis and MacLean (1987) modified Al^{IV}-T empiricism does yield significantly better results than the original function (Cathelineau, 1988, after Cathelineau and Nieva, 1985) or its modification by Jowett (1991).

Agreement between temperatures of chlorite formation calculated using the Walshe (1986) methodology and measured temperatures varies between 15° and 115°C (absolute values of the differences) and is better than 40°C in four of the nine examples considered in Table 3 and Figure 6. This constitutes an improvement on the results of similar comparisons made above for the empirical functions suggested by Kranidiotis and MacLean (1987), Cathelineau (1988), and Jowett (1991). However, the cases where the discrepancies are larger can be used to point to the source(s)

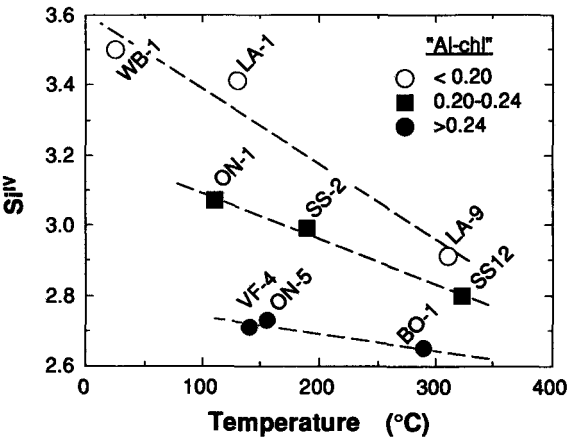

Figure 7. Si^{IV} *vs* temperature plot for the selected chlorites discussed here. Note that the very poor overall correlation is distinctly improved when chlorites of similar Al-content (in terms of "Al-chlorite" end-member proportion) are grouped together. The "Al-chlorite" end-member proportion of a chlorite, as defined in the text, depends on total Al, as well as on Fe and Mg content, and thus is not completely independent of Si^{IV} content. However, the choice of grouping chlorites by "Al-chlorite" end-member proportion here is to permit comparison with Figure 2 and thus illustrate the bulk rock composition/mineralogy effect on chlorite composition.

of the problem(s) currently existing with this approach. The calculated temperatures of formation of chlorite coexisting with quartz, illite and kaolinite in samples ON-5 and VF-4 are 100° and 115°C greater, respectively, than the measured temperature. In contrast, the calculated temperatures of formation of chlorite coexisting with quartz and illite in samples SS-12 and LA-9 are 60° and 100°C less, respectively, than the measured temperature. Overall the results of the tests given in Table 3, together with the results of other, unpublished studies (Walshe, unpublished data) suggest that the Walshe geothermometer works best within a rather narrow range of $a\mathrm{Al}^{3+}/(a\mathrm{H}^{+})^3$ fluid compositions. At temperatures around 300°–350°C, this range of $a\mathrm{Al}^{3+}/(a\mathrm{H}^{+})^3$ fluid compositions lies between the quartz-pyrophyllite buffer and the K-feldspar-muscovite buffer, but does not include the latter buffer. At temperatures around 25°–150°C, the range of $a\mathrm{Al}^{3+}/(a\mathrm{H}^{+})^3$ fluid compositions lies well above the K-feldspar-muscovite buffer. For $a\mathrm{Al}^{3+}/(a\mathrm{H}^{+})^3$ values above the range, the calculated temperatures are too low, and conversely for $a\mathrm{Al}^{3+}/(a\mathrm{H}^{+})^3$ values below the range, the calculated temperatures are too high. The difficulties are an artifact of the activity-composition relations used in the thermodynamic modeling. The idealized activity-composition relations predict minimal compositional changes with respect to changes in the variables $a\mathrm{Mg}^{2+}/(a\mathrm{H}^{+})^2$, $a\mathrm{Fe}^{2+}/(a\mathrm{H}^{+})^2$ and $a\mathrm{Al}^{3+}/(a\mathrm{H}^{+})^3$, and consequently overestimate the variation of composition with temperature (Walshe and Harrold, in prep.).

https://doi.org/10.1346/CCMN.1993.0410210 Published online by Cambridge University Press

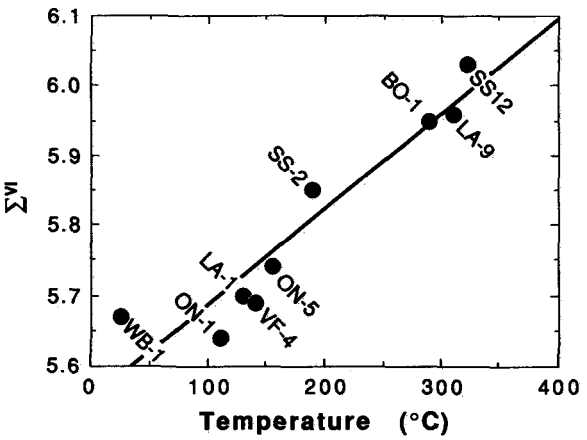

Figure 8. Σ^{VI} *vs* temperature plot for the selected chlorites discussed here. Despite the fact that the correlation coefficient (r^2) of the regression shown is 0.89, preliminary tests indicate that this regression does not have a universal applicability.

The method using intersections between clay-carbonate reactions and CO_2-H_2O miscibility surfaces (Hutcheon, 1990) applied to chlorites from sedimentary basins (samples ON-1, ON-5 and VF-4) yields calculated temperatures of 80°C in all three cases, when appropriate pressure and salinity values are used. These temperatures are lower than present-day formation temperatures at the sampled levels, by a value between 30° and 75°C. The discrepancy may reflect initial formation of chlorite at a relatively low temperature and subsequent growth at progressively higher temperatures. Thus, the resulting chlorite composition would reflect an "average" of the temperature range under which the chlorite precipitated and grew.

It is interesting to notice that, if the data points in Figure 7 are grouped by "Al-chlorite" content, there are three distinct, almost linear, dependencies of Si^{IV} on temperature. (Note that "Al-chlorite" content depends on total aluminum content, and not only on Al^{IV}, which is of course related to Si^{IV}.) The data set used to construct this figure is far too limited to draw any conclusions in terms of new geothermometers, but it appears that, if the "Al-chlorite" mole fraction of a precipitating chlorite is a function of the coexisting mineral phases (bulk rock mineralogy/composition control; see Figure 2), we may expect Si^{IV} to be a different function of temperature in rocks of different mineralogy. Chlorites with the lowest "Al-chlorite" proportions (<0.20) are from samples WB-1, LA-1 and LA-9 and formed within relatively basic rocks (basalt, andesite). From the analogy made above between biotite and chlorite, relatively low "Al-chlorite" proportions are expected for these samples, even if temperature does influence the Al content of chlorite. Chlorites with intermediate "Al-chlorite" proportions (0.20–0.24) are from samples ON-1, SS-2 and SS-12. These samples are from feldspathic sandstones, which are more acidic rock types than basalt or andesite. Chlorites with highest "Al-chlorite" proportions (>0.24) are from samples VF-4, ON-5 and BO-1. The first two samples contain kaolinite (as does sample ON-1), indicating even more acidic bulk rock composition. Sample VF-4 is a quartzose sandstone (Hutcheon, 1990). The third sample, despite containing 0.25 mole proportion of "Al-chlorite," does not coexist with kaolinite, but apparently is found is a very quartzose (acidic) volcanic rock sequence (Lonker *et al.*, 1990).

Figure 8 shows that a relatively good positive correlation exists between Σ^{VI} and temperature for the suite of samples considered here. The calculated regression line has a correlation coefficient (r^2) of 0.89, which is surprisingly good considering the poor overall Si^{IV}-T correlation. Whether Σ^{VI} can be used as a better and more general temperature indicator than Si^{IV}, since it seems to be applicable across a wider range of conditions, is cautioned on the grounds that the calculated regression function from Figure 8 does not necessarily apply satisfactorily to other chlorite composition/temperature data points from the literature. Also, this calculated function, modified to be expressed in terms of octahedral vacancy rather than occupancy, is different than the one found by Cathelineau and Nieva (1985, Figure 10). Therefore, we do not suggest that Σ^{VI} can be used alone as a temperature indicator, despite what comparison of Figures 7 and 8 might at first indicate. The good correlation shown in Figure 8 should be considered as fortuitous at this stage, and, although an increase in Σ^{VI} is generally expected with increasing temperature, this increase may or may not be linear and is likely to be represented by different functions for different bulk rock compositions.

At intermediate temperatures (100°–200°C), some geothermometers seem to display a positive dependency upon Al-content of chlorites (Figure 6). Because Al-content of chlorite is not likely to be a sole function of temperature and will likely also depend, for instance, on coexisting mineral assemblage, no single relationship between Al and temperature should be applied widely. Using the "Al-chlorite" mole proportion as a measure of the Al-content of chlorite minerals has the advantage of considering all Al in the chlorite structure, i.e., both tetrahedral and octahedral Al. From Figure 6, it can be seen that samples ON-1, VF-4 and ON-5, which all have "Al-chlorite" mole proportions in excess of 0.24, yield extremely overestimated calculated temperatures when the Cathelineau (1988) or Jowett (1991) geothermometers are applied. Interestingly, these three samples are the only ones from the selection that contain kaolinite (Table 3), a very aluminous mineral, in the bulk rock mineral assemblage. It should be noted that these samples also have high Fe/(Fe + Mg) values (>0.74). Therefore, the Kranidiotis and MacLean (1987) geothermometer, which has the effect of reducing the calculated temperature as Fe/(Fe + Mg) in-

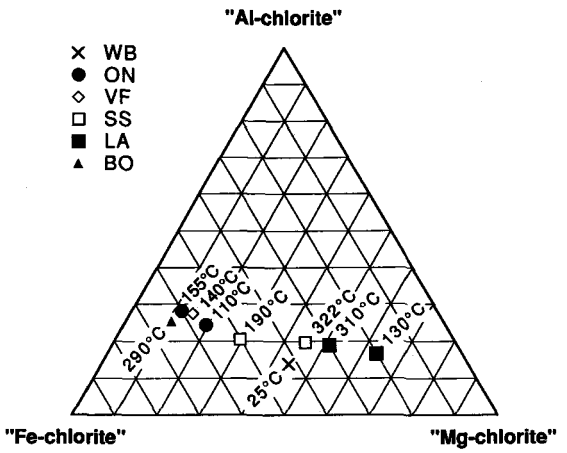

Figure 9. "Al-chlorite," "Fe-chlorite," "Mg-chlorite" ternary diagram constructed as shown in Figure 1, using the end-member proportions calculated in Table 2. All chlorite analyses selected here plot within a broad, near-linear band, but the temperature distribution does not indicate a simple relationship between chlorite composition and temperature of formation over the wide range of conditions presented here.

creases compared to the Cathelineau (1988) function, yields more reasonable temperature estimates in these cases. The high formation temperature of chlorite BO-1, which has a high "Al-chlorite" mole proportion and a high Fe/(Fe + Mg) value, is overestimated by the Cathelineau (1988) and Jowett (1991) functions, and underestimated by the Kranidiotis and MacLean (1987) geothermometer. For samples with lower "Al-chlorite" mole proportions and Fe/(Fe + Mg) values, such as LA-9 and SS-12, the Kranidiotis and MacLean (1987) geothermometer largely underestimates the temperature of chlorite formation, whereas the Cathelineau (1988) and Jowett (1991) functions yield reasonable but meaningless results as they were calibrated partly with these samples.

The composition of the selected chlorites was plotted on an "Al-chlorite," "Fe-chlorite," "Mg-chlorite" ternary diagram (Figure 9) constructed from the tetrahedron of Figure 1. There appears to be a single broad, near-linear band within which all the selected chlorites plot. However, when the temperatures of formation of these chlorites are considered, it is obvious that this trend does not reflect solely a temperature effect. Again, this illustration suggests that the chlorite composition-temperature dependency is very poor for chlorites taken from a variety of settings. The analysis from the weathered basalt, presumably reflecting the composition of a chlorite formed at very low temperature (≈25°C) from a mafic rock (see Eggleton *et al.*, 1987), is adjacent in this diagram to the chlorite with the highest formation temperature (322°C) which formed by hydrothermal alteration of a feldspathic sandstone.

CONCLUSIONS

Attempts to extract temperature information from chlorite has concentrated on two fronts: the structure and the composition of the mineral. Chlorite polytype geothermometry, as it presently stands, is largely qualitative and lacks in-depth investigation of the processes controlling polytype transition. Compositional geothermometry has received much more attention, and several methods of estimating temperature of chlorite formation from chlorite composition have been proposed. The simplest form of chlorite geothermometry consists in calibrating a particular, quantifiable aspect of chlorite composition (e.g., Al^{IV}) with temperature, in a given area where good control exists over temperature and other variables (Cathelineau and Nieva, 1985; Cathelineau, 1988). If this method and the resulting empirical calibration are used to determine temperatures in chlorites from similar settings (bulk rock composition, fO_2, etc.), satisfactory results may be obtained (Bevins *et al.*, 1991). This empirical approach has two important advantages: 1) It takes into account, although not explicitly, the compositional effects of a multitude of thermodynamic variables that do not need to be measured, assuming one can be satisfied that physicochemical conditions of chlorite growth are/were similar to those where the calibration was undertaken; and 2) it is simple to apply, since it generally has the form of a linear function. However, this review shows that these empirical functions appear to be very sensitive to parameters other than temperature (e.g., coexisting mineral assemblage), and their use should not be extrapolated outside the calibration area/conditions without careful evaluation of the impact these parameters may have upon chlorite composition.

As an attempt to account for some aspects of bulk rock composition, several authors have suggested modifications of the empirical geothermometer (Kranidiotis and MacLean, 1987; Jowett, 1991) by which the Fe/(Fe + Mg) value of chlorite, which is directly proportional to that ratio in the bulk rock, is used to correct the Al^{IV}-T dependency. These modified empirical relationships do not, however, appear to be of much wider applicability, as they predict unreasonably high or low temperatures in some of the tested cases.

A different approach was taken by Walshe (1986), whereby the thermodynamic properties of chlorite components were considered in an internally consistent, six-component solid solution model. In this model, the activities of the six chlorite components are calculated from chlorite composition. Assuming the presence of quartz, these activities are then used to derive six unknowns about the physicochemical conditions of chlorite formation: T, aH_4SiO_4, $aAl^{3+}/(aH^+)^3$, $aR^{2+}/(aH^+)^2$, aH_2O and fO_2. This approach is very sensitive to the robustness of the activity-composition

https://doi.org/10.1346/CCMN.1993.0410210 Published online by Cambridge University Press

relations that are used, and application to a selection of chlorite analyses shows that, despite being sometimes out by up to 100°C, it yields temperatures that are the most consistent with measured temperatures, compared with the empirical geothermometers. Work is currently under way to try to incorporate bulk rock compositional effects and $a\mathrm{Al}^{3+}/(a\mathrm{H}^{+})^{3}$ conditions within this geothermometer (Walshe and Harrold, in prep.).

Hutcheon (1990) presented a chlorite geothermometer that relies on the reaction between a carbonate and kaolinite to form chlorite and CO_2. The intersection between the mineral reaction, calculated using the appropriate activities of Fe- and Mg-members for the carbonate and chlorite phases, and the CO_2-H_2O miscibility surface on a temperature *vs* pCO_2 diagram indicates the temperature at which the reaction took place and, hence, at which chlorite is assumed to have formed or started to form. This method requires that the composition of chlorite and the carbonate phase be known and that the fluid not be at, or near, boiling. Preliminary results using this geothermometer under forward modeling conditions indicate that calculated temperature is mostly independent of pressure for cases between the hydrostatic and lithostatic pressure gradients but is rather sensitive to porewater salinity. Because the clay-carbonate chlorite geothermometer of Hutcheon (1990) requires that the fluid be at, or near, saturation pressure with respect to CO_2, this method cannot be used to determine paleotemperatures of chlorite formation in geothermal/hydrothermal systems, but is potentially useful for studies of sedimentary and metamorphic chlorites.

The comparison of the various chlorite geothermometers published in the literature indicates that no single geothermometer performs satisfactorily over a wide range of Al-content, Fe/(Fe + Mg) values, coexisting mineral assemblages, and temperatures. The composition of selected chlorite analyses, together with consideration of stoichiometric observations in biotite minerals, strongly suggests that chlorite composition will not only depend upon temperature but also upon the nature of the coexisting mineral assemblage, or bulk rock composition/mineralogy. This conclusion, reached by few other geothermometry studies (e.g., Velde and Medhioub, 1988), should be stressed, and leads to a cautionary remark to using chlorite geothermometer as a sole method of estimating paleotemperatures, particularly where the effects of bulk rock composition and other thermodynamic parameters upon chlorite composition cannot be precisely evaluated.

ACKNOWLEDGMENTS

The contents of this publication were presented at the 28th Annual Meeting of the Clay Minerals Society held in Houston, October 1991, in the context of the Special Symposium on Clay Geothermometry and Geobarometry. Financial support from the Clay Minerals Society allowing the first author to attend this meeting was much appreciated. A Natural Sciences and Engineering Research Council of Canada (NSERC) Strategic Grant provided a Postdoctoral Fellowship to de Caritat, while an NSERC Operating Grant partly supported Hutcheon's work. Both these sources are gratefully acknowledged. J. L. Walshe acknowledges B. P. Harrold for assistance and the Australian Research Council for financial support. This paper also benefited from the thoughtful reviews by W. L. Huang, J. S. Jahren, and J. R. Glasmann.

REFERENCES

Albee, A. (1962) Relation between mineral association, chemical composition and physical properties of the chlorite series: *Amer. Mineral.* **47,** 851–870.

Angus, S., Armstrong, B., and de Reuck, K. M. (1976) International Thermodynamic Tables of the Fluid State: Carbon Dioxide: *International Union of Pure and Applied Chemistry, Division of Physical Chemistry, Commission on Thermodynamics and Thermochemistry,* Pergamon Press, Elmsford, New York, 385 pp.

Bailey, S. W. (1984) Structures of layer silicates: in *Crystal Structures of Clay Minerals and Their X-Ray Identification,* G. W. Brindley and G. Brown, eds., Mineral. Soc., London (1st reprinting), 1–124.

Bailey, S. W. (1988a) Chlorites: Structures and crystal chemistry: in *Hydrous Phyllosilicates (Exclusive of Micas),* S. W. Bailey, ed., *Reviews in Mineralogy* **19,** 347–403.

Bailey, S. W. (1988b) X-ray diffraction identification of the polytypes of mica, serpentine, and chlorite: *Clays & Clay Minerals* **36,** 193–213.

Bailey, S. W. and Brown, B. E. (1962) Chlorite polytypism: I. Regular and semi-random one-layer structures: *Amer. Mineral.* **47,** 819–850.

Barta, L. and Bradley, D. J. (1985) Extension of the specific interaction model to include gas solubilities in high temperature brines: *Geochim. Cosmochim. Acta* **49,** 195–203.

Bevins, R. E., Robinson, D., and Rowbotham, G. (1991) Compositional variations in mafic phyllosilicates from regional low-grade metabasites and application of the chlorite geothermometer: *J. Metam. Geol.* **9,** 711–721.

Bottinga, Y. and Richet, P. (1981) High pressure and temperature equation of state and calculation of the thermodynamic properties of gaseous carbon dioxide: *Amer. J. Sci.* **281,** 615–660.

Bowers, T. S. and Helgeson, H. C. (1983) Calculation of the thermodynamic and geochemical consequences of nonideal mixing in the system H_2O-CO_2-NaCl on phase relations in geologic systems: Equation of state for H_2O-CO_2-NaCl fluids at high pressures and temperatures: *Geochim. Cosmochim. Acta* **47,** 1247–1275.

Brown, B. E. and Bailey, S. W. (1963) Chlorite polytypism: II. Crystal structure of a one-layer Cr-chlorite: *Amer. Mineral.* **48,** 42–61.

Cathelineau, M. (1988) Cation site occupancy in chlorites and illites as a function of temperature: *Clay Miner.* **23,** 471–485.

Cathelineau, M. and Izquierdo, G. (1988) Temperature-

composition relationships of authigenic micaceous minerals in the Los Azufres geothermal system: *Contrib. Mineral. Petrol.* **100,** 418–428.

Cathelineau, M. and Nieva, D. (1985) A chlorite solid solution geothermometer. The Los Azufres (Mexico) geothermal system: *Contrib. Mineral. Petrol.* **91,** 235–244.

Curtis, C. D., Hughes, C. R., Whiteman, J. A., and Whittle, C. K. (1985) Compositional variation within some sedimentary chlorites and some comments on their origin: *Mineral. Mag.* **49,** 375–386.

De Caritat, P. and Walshe, J. L. (1990) Chlorite geothermometry in low-temperature (diagenetic) investigations: *Geol. Soc. Australia Abstracts* **25,** 284–285.

Deer, W. A., Howie, R. A., and Zussman, J. (1966) *An Introduction to the Rock Forming Minerals:* Longman, London, 528 pp.

Egeberg, P. K. and Aagaard, P. (1989) Origin and evolution of formation waters from oil fields on the Norwegian shelf: *Appl. Geochem.* **4,** 131–142.

Eggleton, R. A., Foudoulis, C., and Varkevisser, D. (1987) Weathering of basalt: Changes in rock chemistry and mineralogy: *Clays & Clay Minerals* **35,** 161–169.

Engel, A. E. J. and Engel, C. G. (1960) Progressive metamorphism and granitization of the Major paragneiss, northwest Adirondack Mountains, New York. Part II: Mineralogy: *Bull. Geol. Soc. Amer.* **71,** 1–58.

Foster, M. D. (1962) Interpretation of the composition and a classification of the chlorites: *U.S. Geological Survey Professional Paper* **414-A,** 33 pp.

Hayes, J. B. (1970) Polytypism of chlorite in sedimentary rocks: *Clays & Clay Minerals* **18,** 285–306.

Hey, M. H. (1954) A new review of the chlorites: *Mineral. Mag.* **30,** 277–292.

Hillier, S. and Velde, B. (1991) Octahedral occupancy and the chemical composition of diagenetic (low-temperature) chlorites: *Clay Miner.* **26,** 149–168.

Hutcheon, I. (1977) The Metamorphism of Sulfide-Bearing Pelitic Rocks from Snow Lake, Manitoba: Ph.D. thesis, Carleton University, Ottawa, Canada, 205 pp.

Hutcheon, I. (1990) Clay-carbonate reactions in the Venture area, Scotia Shelf, Nova Scotia, Canada: in *Fluid-Mineral Interactions: A Tribute to H. P. Eugster,* R. J. Spencer and I-M. Chou, eds., The Geochemical Society Special Publication **2,** 199–212.

Hutcheon, I., Oldershaw, A., and Ghent, E. D. (1980) Diagenesis of Cretaceous sandstones of the Kootenay Formation at Elk Valley (southeastern British Columbia) and Mt. Allan (southwestern Alberta): *Geochim. Cosmochim. Acta* **44,** 1425–1435.

Hutcheon, I., Shevalier, M., and Abercrombie, H. (1993) pH buffering by metastable mineral-fluid equilibria and evolution of carbon dioxide fugacity during burial diagenesis: *Geochim. Cosmochim. Acta* **57,** 1017–1027.

Jahren, J. S. (1991) Evidence for Ostwald ripening related recrystallization of diagenetic chlorites from reservoir rocks offshore Norway: *Clay Miner.* **26,** 169–178.

Jahren, J. S. and Aagaard, P. (1989) Compositional variations in diagenetic chlorites and illites, and relationships with formation-water chemistry: *Clay Miner.* **24,** 157–170.

Jahren, J. S. and Aagaard, P. (1992) Illite-chlorite assemblages in arenite: Chemical evolution: *Clays & Clay Minerals* (in press).

Johnson, J. W., Oelkers, E. H., and Helgeson, H. C. (1992) SUPCRT92: A software package for calculating the standard molal thermodynamic properties of minerals, gases, aqueous species, and reactions from 1 to 5000 bar and 0° to 1000°C: *Computers & Geosciences* **18,** 899–947.

Jowett, E. C. (1991) Fitting iron and magnesium into the hydrothermal chlorite geothermometer: *GAC/MAC/SEG Joint Annual Meeting (Toronto, May 27–29, 1991), Program with Abstracts* **16,** A62.

Karpova, G. V. (1969) Clay mineral post-sedimentary ranks in terrigenous rocks: *Sedimentology* **13,** 5–20.

Kavalieris, I., Walshe, J. L., Halley, S., and Harrold, B. P. (1990) Dome-related gold mineralization in the Pani Volcanic Complex, North Sulawesi, Indonesia: A study of geologic relations, fluid inclusions and chlorite composition: *Econ. Geol.* **85,** 1208–1225.

Kranidiotis, P. and MacLean, W. H. (1987) Systematics of chlorite alteration at the Phelps Dodge massive sulfide deposit, Matagami, Quebec: *Econ. Geol.* **82,** 1898–1911.

Lister, J. S. and Bailey, S. W. (1967) Chlorite polytypism: IV. Regular two-layer structures: *Amer. Mineral.* **52,** 1614–1631.

Lonker, S. W., Fitzgerald, J., Hedenquist, J. W., and Walshe, J. L. (1990) Mineral-fluid interaction in the Broadlands-Ohaaki geothermal system, New Zealand: *Amer. J. Sci.* **290,** 995–1068.

McDowell, S. D. and Elders, W. A. (1980) Authigenic layer silicate minerals in borehole Elmore 1, Salton Sea geothermal field, California, USA: *Contrib. Mineral. Petrol.* **74,** 293–310.

McDowell, S. D. and Paces, J. B. (1985) Carbonate alteration minerals in the Salton Sea geothermal system, California, USA: *Mineral. Mag.* **49,** 469–479.

Muffler, L. P. J. and White, D. E. (1969) Active metamorphism of Upper Cenozoic sediments in the Salton Sea geothermal field and the Salton Trough, southeastern California: *Bull. Geol. Soc. Amer.* **80,** 157–182.

Nockolds, S. R. (1947) The relation between chemical composition and paragenesis in biotite micas of igneous rocks: *Amer. J. Sci.* **245,** 401–420.

Rutherford, M. J. (1973) The phase relations of aluminous iron biotites in the system $KAlSi_3O_8$-$KAlSiO_4$-Al_2O_3-Fe-O-H: *J. Petrol.* **14,** 159–180.

Shirozu, H. and Bailey, S. W. (1965) Chlorite polytypism: III. Crystal structure of an orthohexagonal iron chlorite: *Amer. Mineral.* **50,** 868–885.

Smith, J. T. and Ehrenberg, S. N. (1989) Correlation of carbon dioxide abundance with temperature in clastic hydrocarbon reservoirs: Relationship to inorganic chemical equilibrium: *Mar. Pet. Geol.* **6,** 129–135.

Sourirajan, S. and Kennedy, G. C. (1962) The system H_2O-NaCl at elevated temperatures and pressures: *Amer. J. Sci.* **260,** 115–141.

Takenouchi, S. and Kennedy, G. C. (1965) The solubility of carbon dioxide in NaCl solutions at high temperatures and pressures: *Amer. J. Sci.* **263,** 445–454.

Thompson Jr., J. B. (1982) Composition space: an algebraic and geometric approach: in *Characterization of Metamorphism Through Mineral Equilibria,* J. M. Ferry, ed., Reviews in Mineralogy **10,** 1–31.

Velde, B. and Medhioub, M. (1988) Approach to chemical equilibrium in diagenetic chlorite: *Contrib. Mineral. Petrol.* **98,** 122–127.

Velde, B., El Moutaouakkil, N., and Iijima, A. (1991) Compositional homogeneity in low-temperature chlorites: *Contrib. Mineral. Petrol.* **107,** 21–26.

Walker, J. R. (1989) Polytypism of chlorite in very low grade metamorphic rocks: *Amer. Mineral.* **74,** 738–743.

Walker, J. R. and Thompson, G. R. (1990) Structural variations in chlorite and illite in a diagenetic sequence from the Imperial Valley, California: *Clays & Clay Minerals* **38,** 315–321.

Walshe, J. L. (1986) A six-component chlorite solid solution model and the conditions of chlorite formation in hydrothermal and geothermal systems: *Econ. Geol.* **81,** 681–703.

Weaver, C. E., Highsmith, P. B., and Wampler, J. M. (1984)

Chlorite: in *Shale-Slate Metamorphism in the Southern Appalachians,* C. E. Weaver and associates, eds., Elsevier, Amsterdam, 99-139.

Whittle, C. K. (1986) Comparison of sedimentary chlorite compositions by X-ray diffraction and analytical TEM: *Clay Miner.* **21,** 937–947.

Wiewióra, A. and Weiss, Z. (1990) Crystallochemical classifications of phyllosilicates based on the unified system of projection of chemical composition: II. The chlorite group: *Clay Miner.* **25,** 83–92.

Zen, E.-A. (1959) Clay mineral-carbonate relations in sedimentary rocks: *Amer. J. Sci.* **257,** 29–43.

(Received 18 March 1993; accepted 19 March 1993; Ms. 2354)